Article:

Gomis-Cartesio, LE, Poyatos-More, M, Flint, SS et al. (3 more authors) (2017) Anatomy of a mixed-influence shelf edge delta, Karoo Basin, South Africa. Geological Society Special Publications, 444 (1). pp. 393-418. ISSN 0305-8719

https://doi.org/10.1144/SP444.5

Anatomy of a mixed-influence shelf-edge delta, Karoo Basin, South Africa

LUZ E. GOMIS-CARTESIO[1], MIQUEL POYATOS-MORÉ[1], STEPHEN S. FLINT[1], DAVID M. HODGSON[2], RUFUS L. BRUNT[1] & AND HENRY DE V. WICKENS[3]

[1]*Stratigraphy Group, School of Earth, Atmospheric and Environmental Sciences, University of Manchester, Manchester M13 9PL, UK.*

[2]*Stratigraphy Group, School of Earth and Environment, University of Leeds, Leeds LS2 9JT, UK.*

[3]*Geo-Routes Petroleum, 37 Zevendal Road, Kuils River 7580, South Africa.*

Abstract: The position and process regime of paralic systems relative to the shelf-edge rollover is a major control on sediment transfer into deep water. The depositional strike and dip variability of an exhumed Permian shelf-edge succession has been studied in the Paardeberg Ridge, Karoo Basin. Siltstone-rich slope turbidites are overlain by 25-75 m-thick prodelta parasequences. These are truncated by a 30 m-thick sandstone-prone unit of tabular or convex-topped sandstones, interpreted as wave-modified mouth bars, cut by multiple irregular concave-upward erosive surfaces overlain by sandstones, interpreted as distributary channels. The stratigraphic context, lithofacies, and architecture are consistent with a mixed-influence shelf-edge delta, and the erosional base to the unit marks a basinward shift in facies, consistent with a sequence boundary. Channels become thicker, wider, more erosive, and incise into deeper water facies down dip and correlate to sandstone-rich upper-slope turbidites, all of which support bypass of sand across the rollover. The overall progradational stacking pattern results in a stratigraphic decrease in channel dimensions. Results of this study suggest a predictable relationship between channel geometry, facies and position on the shelf-to-slope profile under a mixed wave and fluvial process regime.

Keywords: *shelf edge, rollover, distributary channel, reworked mouth bars, Karoo Basin*

Basin margin progradation and the timing of sediment transport to the oceans is strongly influenced by the position and character of paralic systems relative to the physiography of the shelf-edge rollover (e.g. Edwards 1981; Mayall *et al.* 1992; Sydow & Roberts 1994; Morton & Suter 1996; Steel *et al.*

2000; Muto & Steel 2002; Porębski & Steel 2003; Steel *et al.* 2003; Saller *et al.* 2004; Carvajal & Steel 2009; Covault *et al.* 2009; Dixon *et al.* 2012a). The presence of gullies and channels, which incise into shelf-edge deltas and act as conduits for sediment transport, have been widely described and associated with multiple factors, including lowering of relative sea level, headward erosion of submarine canyons, gravitational instabilities and slope failure, gravity flows and/or high fluvial discharge, among others (e.g. Pratson *et al.* 1994; Fulthorpe *et al.* 1999, 2000; Muto & Steel 2002; Plink-Björklund & Steel 2002; Donovan 2003; Porębski & Steel 2003; Posamentier & Kolla 2003; Petter & Steel 2005; Plink-Björklund & Steel 2005; Jackson & Johnson 2009; Sanchez *et al.* 2012b; Sylvester *et al.* 2012; Prélat *et al.* 2015).

In contrast to reflection seismic data, exhumed shelf-margins provide the resolution needed to constrain the interplay of sedimentary processes responsible for channel and gulley initiation at the shelf-edge rollover (Hubbard *et al.* 2010). Typically, however, shelf-edge deltas are interpreted to be dominated by a particular process regime (Dixon *et al.* 2012b). Mixed-influenced systems are rarely reported (Mellere *et al.* 2003; Pontén & Plink-Björklund 2009; Bowman & Johnson 2014), and the fine-scale down dip changes in channel geometry and infill architecture across the shelf-edge rollover have not been documented at outcrop. Most published examples of exhumed rollovers are from high-gradient shelf margins with short slope lengths (Pyles & Slatt 2000; Mellere *et al.* 2002; Plink-Björklund & Steel 2005; Carvajal & Steel 2006; Pyles & Slatt 2007; Pontén & Plink-Björklund 2009; Helland-Hansen 2010). This contrasts with the generally low gradients observed in many seismic datasets (e.g. Pirmez *et al.* 1998; Cattaneo *et al.* 2007; Patruno *et al.* 2015) that are challenging to constrain at outcrop (e.g. Dixon *et al.* 2012a; 2012b; Jones *et al.* 2013).

The importance of lateral variability in shelf margin physiography, and distribution of erosional and depositional process regimes, is highlighted in modern (e.g. Olariu & Steel 2009) and three-dimensional reflection seismic datasets (e.g. Suter & Berryhill 1985; Matteucci & Hine 1987; Poag *et al.* 1990; Tesson *et al.* 1990; Milton & Dyce 1995; Fulthorpe & Austin 1998; Kolla *et al.* 2000; Saller *et al.* 2004; Hadler-Jacobsen *et al.* 2005; Crumeyrolle *et al.* 2007; Ryan *et al.* 2009; Henriksen *et al.* 2011; Moscardelli *et al.* 2012; Sanchez *et al.* 2012a, b; Bourget *et al.* 2014). Outcrop studies focus on determining clinoform and rollover geometries down depositional-dip profiles (e.g. Steel *et al.* 2000; Plink-Björklund & Steel 2002; Mellere *et al.* 2003; Plink-Björklund & Steel 2005; Pyles & Slatt 2007;

Uroza & Steel 2008; Dixon *et al.* 2012a). Documented outcrop examples with large-scale along-strike control are rare (e.g. Dixon *et al.* 2012a; Jones *et al.* 2015).

In this study, a rare example of an exhumed paralic succession in a shelf-edge rollover position with extensive depositional-strike and dip constraints is presented from the Permian Waterford Formation in the Tanqua depocentre, Karoo Basin, South Africa. The outcrops permit the following objectives to be addressed: i) to describe the vertical transition from slope to shelf deposits and to identify the shelf-edge rollover and ii) to discuss the origin, evolution and infill of channel-form features across the slope to shelf transition.

Geological setting

The Late Carboniferous-Triassic Karoo Basin (Fig. 1) has been interpreted as a retroarc foreland basin with subsidence caused by flexural loading by the Cape Fold Belt (Johnson 1991; Cole 1992; Visser 1993; Veevers *et al.* 1994; Catuneanu *et al.* 1998). However, more recent studies have suggested that subsidence was due to long wavelength dynamic topography effects driven by the subducting palaeo-Pacific plate (Tankard *et al.* 2009). The fill of the Karoo Basin comprises the 5+ km thick Karoo Supergroup (Smith 1990) (Fig. 2a). Glacial deposits of the late Carboniferous Dwyka Group are overlain by Ecca Group post-glacial strata of the Prince Albert, Whitehill, and Collingham formations, which show a deepening trend from shallow water carbonates to basin plain turbidites (De Beer 1992; Turner 1999; Johnson *et al.* 2006). In the Tanqua Depocentre, the Collingham Formation is overlain by ~800 m of mudstones of the Tierberg Formation (Fig. 2a). Overlying these mudstones, the Skoorsteenberg Formation comprises sandstone-rich basin-floor fans 1-4 (Bouma & Wickens 1991; Wickens 1994; Scott *et al.* 2000; Johnson *et al.* 2001; Andersson *et al.* 2004; Hodgson *et al.* 2006), overlain by a channelised slope wedge of Unit 5 (Wild *et al.* 2005). These deposits are topped by slope to shelf sediments of the Kookfontein and Waterford formations (Wickens 1994; Wild *et al.* 2009; Oliveira *et al.* 2011; Dixon *et al.* 2012a; 2012b, here all referred to as the Waterford Fm.), which are the focus of this study (Fig. 2).

Dataset and methods

The Waterford Formation crops out across the north-eastern part of the Tanqua depocentre, providing a study area of up to ~1600 km^2. This study is focused on the Paardeberg Ridge locality (Fig. 1b), which exposes the stratigraphic transition from slope to shelf deposits (Fig. 2b) over an area of up to 10 km^2. The outcrop (Fig. 1c) is a 150 to 400 m-high, 5 km-long NW-SE trending ridge with a steep SW face and gullied NE face that provides good three-dimensional control (Fig. 1c). The overall tabular and laterally continuous succession has been informally divided into lower, middle and upper units (Fig. 2b and 3). The 30-40 m thick sandstone-rich middle unit displays a complex assemblage of tabular or convex-topped sandstones cut by irregular concave-upward erosive surfaces overlain by sandstones, and is the main focus of this study.

Four regional (1:50 scale) sedimentary logs (DRs, DR1, DR6 and OUS) provide the general stratigraphic context and are combined with 10 detailed logs (1:25 scale), focused on the middle unit, to characterise the different erosional and depositional features in each locality (1090 m of cumulative logged thickness). Physical correlation of stratigraphic units was constrained by walking out key surfaces between logs, on both faces of the ridge and in intervening areas to map and capture depositional dip and strike changes in facies and geometries. All observations were recorded on high-resolution photo-panels, satellite imagery and aerial photographs (Fig. 1c and 3). Palaeocurrent measurements (n=670) were taken from planar and trough cross-bedding foresets, ripple-cross lamination, primary current lineation, basal tool marks and channel-margin orientations (Fig. 4). A stratigraphic hierarchy based on lithofacies, palaeocurrent measurements and key surfaces was developed to capture the stacking patterns across multiple scales and to understand the temporal changes in erosion and deposition.

Facies analysis

Lithofacies have been defined based on lithology, grain size, and sedimentary structures in Table 1 and are interpreted in terms of depositional processes. Facies associations are described using lateral and vertical relationships, and interpreted in terms of different depositional environments.

Lithofacies

A primary classification is based on three main facies groups, according to the maximum grain size observed within single beds (Table 1 and Fig. 5): conglomerate (C); sandstone (S) and mudstone (M); the latter includes the spectrum of grain populations from coarse silt to clay.

Facies associations

FA-1: Diffuse laminated to structureless mudstones. Dark grey to green fissile to blocky mudstone bed sets. Commonly structureless fine-medium siltstone (*Md, Mo*), interbedded with coarse-siltstone beds (*Ms*) with occasional parallel lamination, isolated/starved mm-scale ripples or gently undulating lamination. Bioturbation is low to moderate.

These facies are interpreted to represent deposition from suspension fallout, although some of their coarser and laminated components indicate deposition from dilute turbidity currents (Macquaker & Bohacs 2007; Schieber *et al.* 2007). The depositional environment is interpreted to record offshore deposition below storm wave base on the outer shelf or upper slope (Wild *et al.* 2009; Jones *et al.* 2013). This facies association forms the bulk of the strata in the lower part of the regional succession (lower unit).

FA-2i: Heterolithic siltstone-prone thin beds. Thin- to very thin-bedded (cm- to mm-scale) planar and current-ripple cross-laminated siltstone (*Ms*), interbedded with minor amounts of ripple-laminated (unidirectional or bidirectional) very fine-grained sandstones (*Sr, Sw*), which commonly show inverse- to normal-graded composite beds (*Sg*). These deposits can form laterally extensive tabular packages (several hundred metres) or wedges of slightly inclined strata (a few tens of metres) that drape and/or onlap erosion surfaces. Bioturbation is low to moderate, and the presence of organic debris is common.

This facies association is interpreted to record either deposition from low-concentration turbulent suspension flows that developed distally or laterally from denser hyperpycnal flows (Plink-Björklund & Steel 2004; Bhattacharya & MacEachern 2009; Zavala *et al.* 2011), or deposition from dilute turbidity currents in unconfined settings. This facies association has been interpreted to reflect deposition in a distal prodelta/offshore transition environment relatively far from the sediment feeder system, but still recording the effects of waves.

FA-2ii: Heterolithic sandstone-prone thin beds. Laterally-extensive (up to several hundreds of metres) 1 to 15 m-thick packages of thin-bedded (cm-scale) parallel or ripple-laminated, inverse or normal graded, very-fine grained sandstone *(Sl, Sr, Sw)* alternating with planar- and current ripple-laminated siltstone *(Ms)*. Locally, erosional bed bases and inverse grading are observed in thin sandstone beds, and ripple-lamination includes asymmetrical, combined or symmetrical forms. In places, this facies association includes medium- to thick-beds (up to 50 cm) of partially amalgamated, fine-grained sandstone *(Ss, Sg, Sl)* forming lenticular packages. Bioturbation is moderate to high, and the presence of unclassified organic fragments is common.

This facies association is interpreted to record the deposits of moderate- to low-concentration turbidity currents in both confined (within erosive surfaces) and unconfined settings (tabular and laterally extensive packages). Commonly, the association passes laterally into silt-prone heterolithic deposits *(FA-2i)*, and suggests deposition in a proximal prodelta/shoreface-offshore transition setting (Hampson 2000; Hampson & Howell 2005). The local thicker sandstone beds reflect deposition from rapidly expanding, energetic turbulent suspension flows. This facies association can also be found in marginal or upper parts of channelised elements (Fig. 3b and 6).

FA-3i: Thin- to medium-bedded sandstones. Laterally-persistent parallel-sided, fine-grained sandstone bedsets intercalated with thinner very-fine grained sandstone bedsets. Beds are up to 20 cm-thick. Some beds are normally or inversely graded (*Sg*), without structures, but most of them show a range of sedimentary structures including parallel lamination (*Sp,* Fig. 5e), trough cross-bedding or low angle or hummocky cross-stratification (*Sx, Sl,* Fig. 5e-f), and bed tops exhibit both symmetrical and asymmetrical ripple forms (*Sr, Sw,* Fig. 5g-h). Climbing-ripple cross-lamination is common. Bioturbation is generally from moderate to high, and organic fragments are commonly observed in bedding planes.

Normal and/or inverse graded beds are interpreted to represent deposition from river-derived waning and/or waxing sediment-laden flows, respectively (e.g. Mulder *et al.* 2003; Plink-Björklund & Steel 2004; Petter & Steel 2006; Olariu *et al.* 2010). The structured beds indicate tractional reworking by high concentration flows and, in the case of climbing ripples, high sedimentation rates possibly associated with abrupt decrease in flow confinement.

The depositional environment of *FA-3i* is interpreted depending on the dominance of particular sedimentary structures. The planar, trough and climbing ripple cross-lamination facies association is related to deposition from unidirectional flows in distal mouth bars. Where low-angle, HCS-swaley cross-stratification in cleaner sandstones predominates, deposition is interpreted to be in a distal wave-influenced delta front or lower shoreface setting (e.g. Hampson 2000; Bhattacharya & Giosan

2003; Hampson & Howell 2005). Thin-bedded sandstones are also observed in marginal or upper parts of channelised bodies (Fig. 3b & 6).

FA-3ii: Medium- to thick-bedded sandstones. Laterally extensive or channelised, very fine- to fine-grained, predominantly structureless or graded sandstone (*Ss, Sg,* Fig. 5c-d) bedsets, contain amalgamation surfaces, scattered mudstone clasts (*Cm,* Fig. 5b), and fluid-escape structures. Structureless divisions can pass upward into thick-bedded parallel laminated (*Sp,* Fig. 5e) or very low angle cross-laminated sandstones (*Sl*), which in turn pass upward into asymmetrical or symmetrical ripple-laminated thick-bedded sandstones. Laterally, bedsets either onlap directly onto inclined erosional surfaces or pass laterally into thin-bedded sandstones (*FA-3i*) or interbedded sandstones and siltstones (*FA-2*). In channelised examples, the lower part of this facies association usually includes intraformational pebble-size mudstone clasts in irregular horizons of clast-supported conglomerate to sandy matrix-supported conglomerate in a sandy matrix (*Ci*). Bioturbation is highly variable, from low to high, and organic fragments in bedding planes can be present.

The nature of the structureless or graded sandstone beds suggests rapid deposition and frictional freezing from high-density sediment gravity flows with a high fallout rate that prevents bedload transport and traction in the base of the flow (e.g. Mutti *et al.* 2003; Tinterri 2007). Basal mudstone clast horizons are residual lag deposits of material eroded and left behind by largely bypassing flows (Stevenson *et al.* 2015). Parallel laminated beds could be associated with upper-flow-regime plane bedding or downstream migration of very low-amplitude long-wavelength bedforms, as has been described in younger fluvial deposits of the Beaufort Group (Turner 1981; Stear 1983; Stear 1985; Wilson *et al.* 2014). Cross- and ripple-laminated beds indicate aggradation and traction processes. This facies association suggests relatively high-energy depositional environments and is found either filling central parts of concave-up erosion surfaces (scour- or channel-fills), or in the upper part of lenticular/tabular elements interpreted as mixed-influenced proximal mouth bars (Fig. 3b and 6).

FA-4: Deformed facies associations. Laterally discontinuous packages of folded and distorted sandy or silty thin- (*FA-1, 2*) to thick-beds (*FA-3*) that can extend laterally for several hundred metres. They show a wide spectrum of soft-sediment deformation types, ranging from complete destruction of primary sedimentary structures and contorted sandstone clasts floating in a sandy/silty matrix, to units with coherent upward directed folds in sandstones. They usually contain large-scale (<5 m-high) fluid-escape structures and commonly occur associated with erosional and irregular surfaces.

Depending on the original structures and relative stratigraphic position, deformation is interpreted to record a spectrum of processes, from *in-situ* foundering to remobilisation (Owen 2003; Wild 2005; Wild *et al.* 2009; Oliveira *et al.* 2011; Jones *et al.* 2013), related to failure or gravitational collapse in oversteepened delta front or channel margin settings. These deposits represent approximately 30% of the middle unit and are also present in the lower part of the upper unit (Fig. 2b, 3b and 6).

Stratigraphic evolution

The lower Waterford Formation in the study area is informally divided into lower, middle, and upper units (Figs.2 and 3). The lower unit succession starts with a 30-40 m-thick dark grey mudstone (*FA-1*), with some isolated sandstone bedsets up to 3 m-thick (*FA-3ii*). This is overlain by four 20 to 75 m-thick heterolithic coarsening- and thickening-upward packages (FA-1 to FA-2ii), each starting with a regionally extensive mudstone (FA-1). The succession is abruptly overlain by the 30 m thick middle unit, which comprises tabular or convex-topped deformed sandstones incised by multiple erosive surfaces overlain by sandstones (FA-2 and FA-3). The middle unit is capped by a 2 m thick regionally extensive mudstone (Fig. 3b), above which the upper unit comprises thinner (10-50 m) sandier and deformed coarsening- and thickening-upward packages with progressively lower mudstone content. These packages are overlain by a mudstone-dominated unit, with relatively isolated sandstone beds or bedsets that are either tabular or channelised (*FA-3i* and *FA3-ii*). A gradual change in colour from dark grey to green and purple is observed in the uppermost mudstones.

The basal mudstone-prone lower unit with intercalated sandstone beds is interpreted as slope mudstones and turbidites. The overlying four coarsening- and thickening-upward heterolithic packages of the lower unit are interpreted as dominated by prodelta and offshore deposits. The vertical profile and the scale of these stratigraphic packages are consistent with parasequences bounded by flooding surfaces as described by Van Wagoner *et al.* (1990), and their stratigraphic setting is consistent with an upper slope position. This parasequence set is overlain abruptly by erosional channel-fills and deformed lobate bodies (mixed-influence mouth bars) of the middle unit, described and interpreted in detail below. The regional capping mudstone is interpreted as containing a flooding surface. The sandier, thinner and deformed deposits of the upper unit are interpreted as wave-dominated or mixed-influenced shelf delta/shoreface parasequences (Wf of Ainsworth *et al.* 2011). These are overlain by isolated fluvial sandstone bodies within grey-green and purple floodplain mudstones of the lower Beaufort Group (Wilson *et al.* 2014).

Palaeocurrent analysis and palaeoshoreline orientation

Palaeocurrent analysis in this study, combined with previous publications on the Waterford Fm. and underlying submarine fan systems in the Tanqua depocentre, indicate a uniform regional palaeoflow to the NE and N, with a slope and overlying shelf oriented approximately NW-SE (Johnson *et al.* 2001; van der Werff & Johnson 2003; Wild *et al.* 2005; Hodgson *et al.* 2006; Luthi *et al.* 2006; Wild *et al.* 2009; Jones *et al.* 2013). In the mud-prone lower unit (*FA-1*), there is a general E-to-NE unidirectional palaeoflow, with an E-W trend from symmetrical ripples in sandstone beds (Fig. 4a). The overlying parasequences show a N-to-NE spread in unidirectional current ripples and a NE-SW trend for the bidirectional indicators (Fig. 4a). All this evidence suggests that the NW-SE orientation of the Paardeberg Ridge outcrop is a strike section to the palaeoshoreline and shelf-edge during progradation of the basin margin (Fig. 7).

Depositional elements in the middle unit

Architectural descriptions of the Paardeberg Ridge exposure (Fig. 3) are focused on the sandstone-dominated middle unit, which is characterised by two geometries: channelised and lobate.

Channelised bodies

In cross-section (Fig. 3), these bodies have basal concave-up surfaces (Fig. 6) that truncate underlying deposits with up to 20 m of incision. Individual channel bodies (Table in Fig.6) range from 5 to 20 m-thick and 50 to 400 m-wide which, given the strike orientation of the outcrop, are close to true widths. They can be followed, in planform view (Fig. 7), for up to 350 m down dip where they increase in width and thickness downdip. Commonly, they are cut by younger erosion surfaces, so that only remnant fills are preserved (Fig. 6). Where fully preserved, cross-sectional geometries range from symmetric (Fig. 6) to asymmetric with one steeper erosive side and the other side showing a low angle contact and a lateral facies change (Fig. 3b and 6). Loaded or slightly deformed bases and abundant mudstone-clast conglomerates close to erosional bases are common (Fig. 3b and 6).

Facies associations within channelised bodies stack to form fining- and thinning-upward packages (Fig. 8), which in most cases also fine and thin laterally (Fig. 6). Packages have basal mudstone-clast conglomerates (Fig. 5a-b) overlain by thick-bedded structureless sandstones (*FA-3ii,* Fig. 5c) that grade vertically and laterally into parallel-laminated (Fig. 5e) or very low angle laminated thick-bedded sandstones (*FA-3ii*). These deposits pass gradually upward into thin-bedded sandstones (<30 cm; *FA-3i*), which in turn may grade vertically and laterally into interbedded sandstones (up to 15 cm-thick) and siltstones (*FA-2ii* and *FA-2i*), with a gradual decrease in sandstone content (Fig. 6 and 8). Sandstones in the thin-bedded and interbedded packages are either structureless, parallel-laminated or with symmetrical and asymmetrical ripple cross lamination and commonly show symmetrical rippled tops.

These bodies are interpreted to be channel deposits, showing multiple phases of cut and fill. Their facies associations and position are consistent with subaqueous distributary channels in a deltaic setting but, their scale, localisation and the processes responsible for their origin and fill are discussed below.

Lobate bodies

These bodies are generally lens-shaped in cross-section with irregular bases (deformed or slightly erosive) and flat to convex-up tops, although cross-sectional geometry can be modified by subsequent channel erosion (Fig. 3 and 6). Axes comprise fine-grained sandstone thinning laterally into finer grained facies. Lobate bodies (Table in Fig.6) range from 5 to 10 m-thick and from 75 to 600 m-wide (true width) and have been mapped for up to 300 m down dip (Fig. 7). Typically, they overlie thinner, off-axis parts of older lenticular bodies (Fig. 6) or previously deposited channelised elements (Fig. 6), indicating a compensational stacking pattern (Fig. 3b).

Facies associations in lobate bodies stack in coarsening- and thickening-up packages (approx. 15m-thick) (Fig. 6 and 8). Commonly, a lower section of sand-prone interbedded siltstones and sandstones (*FA-2ii*) coarsens upwards into thin-bedded sandstone (*FA-3i*). Sandstone beds are normally graded with parallel lamination and both asymmetrical and symmetrical ripple lamination. Most bed tops show symmetrical ripples. Towards the upper part of the bodies soft-sediment deformed packages (*FA-4;* Fig. 8) show slightly erosive, heavily distorted or loaded bases (Fig. 6). Where primary fabric is preserved, in most cases it is thick-bedded sandstone (*FA-3ii*) and/or interbedded sandstone and siltstone (*FA-2i* and *FA-2ii*). Flames and other fluid escape structures at loaded bed bases can reach up to 4 m-high. Thin to thick-bedded sandstones with abundant climbing ripple lamination (*FA-3,* Fig. 5f) are commonly found above, below or between deformed deposits, sometimes eroding the underlying deformed deposits, or in blocks within the deformed packages.

The mixed process origin with indicators of both river- and wave-regime, and widespread soft-sediment deformation in these lenticular sandstone bodies makes them challenging to assign a simple interpretation. However, the modified coarsening-upward trends with unidirectional currents, with reworked bed tops, and the close association with subaqueous distributary channels, leads us to interpret and refer to them as mixed-influence (wave and river) and remobilised mouth bars that were reworked into more strike elongate lobate geometries.

Architecture and stratigraphic evolution of the middle unit

Cross-cutting relationships between sedimentary bodies allow reconstruction of the relative ages of the channelised and lobate deposits (tx_C or tx_L respectively in Fig. 3) and therefore the stratigraphic evolution of the middle unit to be interpreted.

The architecture suggests a spatial relationship between the underlying deposits and the positioning of younger elements. Superposition of channels and mixed-influence mouth bars follows a complex temporal distribution (Fig. 3), consistent with lateral compensation processes. Combined with the facies associations, the architecture could also indicate the proximity to an input point at this locality (Olariu & Bhattacharya 2006; Olariu & Steel 2009).

In general, the older channelised elements are sandier, with more structureless sandstone, and wider (Fig. 3b and 6) than the younger channels. Commonly, they cut into deeper water offshore facies and also locally into prodelta and/or deformed mixed-influence mouth bars (Fig. 3b). Most of these older channels show multiple scours with abundant mudstone clast lags (Fig. 3b and 6), which may suggest recurrent erosion processes and sediment bypass at the same location over time. Younger channels display a wider spectrum of facies associations, and are generally narrower with simpler cuts (Fig. 6). Cleaner basal surfaces, less amalgamation, and considerably less mudstone clast lags at their bases are consistent with less erosive and shorter-lived channels. Typically, these younger channels cut shallower water facies associations (deformed mixed-influence mouth bars) and their fills show a greater degree of wave reworking towards their tops, suggesting deposition in a shallower water setting.

Lateral and vertical relationships between depositional elements

Typically, a lobate element (or mixed-influence mouth bar) is cut or partially eroded by a channelised element (Fig. 6 and 8). The basal incision surfaces of channelised bodies usually cut from the top of the underlying lobate element. The presence of collapsed mixed-influence mouth bar facies in channel-fills has been locally observed (Fig. 8 and 9) indicating that channels were open conduits and suggesting a close relationship between mouth bar deposition and channel forming processes (Olariu & Bhattacharya 2006). Channelised bodies are in turn overlain by younger lobate elements, and this pattern is repeated vertically and laterally along the outcrop.

Palaeocurrents in the middle unit

In channelised bodies, unidirectional measurements from current and climbing ripples, low angle cross bedding, and basal groove marks show a dominant NE and N trend, with a dispersion of up to 90° (Fig. 4a & b). Orientation of channel margins support the general SW to NE trend (Fig. 7). Current ripple lamination from channel margin thin beds show a NE trend, and symmetrical ripples are oriented NE-SW (Fig. 4b), consistent with the regional wave reworking measurements (Fig. 4a). Palaeocurrents in the mixed-influence mouth bars or lobate elements show a similar bidirectionality (NE-N to SW-S) but the unidirectional measurements show a dominant northward trend with a spread of 90° (Fig. 4c). Orientations from the upper parts of mixed-influence mouth bars or lobate elements show a wider spread than the lower parts (Fig. 4c). The consistent unidirectional NE trends, and the dominant, consistent NE-SW (040°-220° to 080°-260°) trend of bidirectional measurements from symmetrical ripple crest lines (Fig. 4d) supports the overall NW-SE shoreline orientation.

Discussion

A mixed-influence shelf-edge delta

The Paardeberg Ridge locality lies 15 km down dip of, and approximately 200 m stratigraphically above the well documented Tanqua deepwater succession, which comprises basin floor fans 1-4 (Wickens 1994; Hodgson *et al.* 2006) and the Unit 5 lower slope turbidite succession (Wild *et al.*

2005). This regional framework provides an upper slope stratigraphic context for the lower unit of the Paardeberg Ridge (mudstones and 20-75 m thick parasequences dominated by thin bedded heterolithics). The thinner (10-25 m), sandier parasequences of the upper unit, with common occurrence of HCS and symmetrical ripples, are interpreted as wave dominated and mixed-influenced shelf parasequences and share many characteristics with the Waterford Formation in other parts of the basin-fill (Wild *et al.* 2009; Jones *et al.* 2013, 2015). The sandstone-rich middle unit, which separates the underlying upper slope from overlying shelf deposits, marks an abrupt increase in the amount of erosion and soft-sediment deformation, with proximal facies associations of sandstone-rich mixed-influence mouth bars (*FA-3*) cut by sandstone-rich distributary channel-fills (*FA-2* and *FA- 3*). The stratigraphic context, combined with facies analysis and palaeocurrent data, supports the interpretation of the middle unit as a shelf-edge deltaic package that formed during progradation towards the NE. The Karoo palaeo-shelf margin is generally considered as a low gradient (Wild *et al.* 2009), stable slope type (*sensu* Ross *et al.* 1994), with limited syn-sedimentary growth faulting (Jones *et al.* 2013), and widespread amount of soft-sediment deformation and localised slumps (Wild *et al.* 2009; Oliveira *et al.* 2011; Jones *et al.* 2013).

The fill of channelised elements in the middle unit commonly comprises thick-bedded structureless axial sandstones that pass laterally through thin-bedded sandstones to interbedded channel margin sandstones and siltstones (Fig. 6 and 8). Bed tops with symmetrical ripples following the regional NE-SW palaeocurrent trend are found in the thin-bedded channel margin and uppermost parts of the channel fills. While large storm waves can rework the sea floor at water depths greater than 100 m the ubiquity of symmetrical ripples and consistency of palaeocurrents indicate deposition above fair weather wave base during channel filling. The thickness and generally structureless character in axial to marginal thick-bedded deposits suggest high-energy conditions, but dune-scale bedforms in channelised elements are rare. This paucity of cross-bedding can be attributed either to unusually high discharges during short, temporary flash-flood events (Stear 1983) or to the inhibition of bedform formation due to the narrow grain size range (clay to fine sand) in the whole Karoo Basin (Southard 1971; Turner 1981; Van den Berg & Van Gelder 1993), which constrains the spectrum of possible sedimentary structures to lower and upper phase plane bedding, and ripples (Rubin & McCulloch 1980; Southard & Boguchwal 1990). Low-angle cross-stratification is locally observed, and has been associated with very low-amplitude unidirectional bed forms (e.g. Turner 1981; Stear 1983; 1985;

Wilson *et al.* 2014), but also to combined-flow structures such as hummocky cross-stratification (Nøttvedt & Kreisa 1987; Southard *et al.* 1990). However, its expression is difficult to recognize and interpret in the absence of a wider grain size range. The facies and architectural elements of the studied succession suggests that different process regimes coexisted at the same location during clinothem progradation, and as such is a rare example of an exhumed mixed-influence shelf-edge system. Mixed-influence shelf-edges have been observed in modern systems (e.g. Ainsworth *et al.* 2011; Olariu 2014), and in a few studies of ancient shelf margins (e.g. Olariu *et al.* 2012; Sanchez *et al.* 2012b; Jones *et al.* 2015).

Relative sea level at the shelf edge

Parasequences of the lower unit show an overall progradational trend (DRs in Fig. 1b and DR1, DR6 and OUS in Fig. 10). The highly tabular character (Fig. 3a) and absence of lateral compensational stacking are interpreted to record relatively high accommodation conditions on the upper slope-lower unit (Wild *et al.* 2009). The sharp and erosional basal contact of the sand-rich middle unit, with its mixed-influence mouth bar and distributary channels directly truncating upper slope thin beds (Fig. 1b, 3b and 10), indicates a basinward shift of the facies belt. Highly erosive elements and evidence of sediment instability, the multi-storey stacking and limited thickness (approx. 30 m; Fig. 3b) of the middle unit are consistent with an abrupt change into a more proximal facies succession in a lower accommodation setting.

The abrupt change in depositional environments and stacking patterns in the middle unit does not support a simple progradational trend, which would display a gradual upward increase in sandstone content of parasequences as the delta approached the shelf edge. The basal erosion surface ($t1_C$; Fig. 3b) of the middle unit is therefore interpreted as a sequence boundary (sensu Posamentier *et al.* 1988), juxtaposing a paralic succession onto the shelf edge rollover as a response to a relative fall in sea level. No palaeosol deposits, roots or desiccation cracks have been found to indicate subaerial exposure of the shelf edge, which suggests that shelf edge accommodation was reduced but remained subaqueous. A similar situation has been documented in the Laingsburg depocentre by Jones *et al.* (2013), who interpreted this absence of subaerial exposure as consistent with a Type 2 sequence boundary (sensu Posamentier *et al.* 1988). Correlation of the middle unit 1-3 km down dip to the Ouberg Pass area (Fig. 10) has revealed a succession of sandstone-dominated turbidites, which are interpreted to represent significant sediment bypass through the shelf edge rollover channels. The flooding surface overlying the middle unit (Fig. 3b) marks a relative rise in sea level. Sufficient new accommodation was subsequently generated on the shelf to allow deposition of shelf parasequences of the upper unit, which are thinner, sandier and display shallower facies associations than those of the lower unit (Fig. 1b and 3a).

Shelf-edge channel geometry and initiation mechanisms

Additional evidence of a shelf-edge rollover setting is derived from mapping (Fig. 7) and correlation between the two sides of the Paardeberg Ridge, which provides a planform control (100 to 350 m dip section) for the channelised elements of the middle unit (Figs. 7 and 9). Channels are thicker, more incised, with a greater amount of mudstone clast lags and soft sediment deformation on the down dip north-eastern side of the ridge than on the up dip south-western side (Fig. 9). On the up dip side of the ridge, channels cut deformed mixed-influence mouth bar deposits (Figs. 3b and 9) or older channel fills while on the down dip side they also cut down into prodelta and offshore deposits. This basinward increase in channel dimensions and depth of erosion is interpreted to reflect the increased gradient and accommodation across the shelf-edge. The steeper gradient enhances the depth of erosion of distributary channels (Olariu & Bhattacharya 2006; Jackson & Johnson 2009), and the onset of gravity driven density flows and gravitational collapse of channel margins across the rollover (e.g. Bowman & Johnson 2014) (Figs. 10 and 11). Residual deposits, amalgamation surfaces and multi-storey stacking in the channels of the middle unit suggest relatively long-lived sediment bypass. This is consistent with the existence of a gullied/scoured slope. Two kilometres farther down dip (NE of the Paardeberg ridge; Figs. 1c and 10) the prodelta-offshore succession is abruptly overlain by thick-bedded (0.5-1m thick) normally graded sandstones that pass from structureless to climbing ripple cross laminated. The beds are lens shaped with erosional bases and sole marks oriented NE-SW (parallel to the main palaeocurrent direction). These deposits are interpreted as turbidites, and the basinward upper slope expression of the middle unit (Figs. 10 and 11).

Although erosional features and sediment conduits (channels and gullies) are commonly observed at the shelf edge rollover (e.g. Porębski & Steel 2003; Sylvester *et al.* 2012; Bowman & Johnson 2014; Prélat *et al.* 2015), the processes involved in their origin require a wide range of possibilities to be considered. Several mechanisms of subaqueous scouring on the outer shelf region are rejected due to the scale and orientation of the incisions or the latitude of the basin at that time (between 40-60º degrees south, Faure & Cole 1999). These include glacial scouring or bottom currents from melting (e.g. Ridente *et al.* 2007), longshore currents (e.g. Lewis 1982; Galloway 1998; Mazières *et al.* 2013), shallow-water bottom currents (e.g. Viana *et al.* 2002), and density cascades (e.g. Wilson & Roberts 1995; Shapiro & Hill 1997; Ivanov *et al.* 2004). Erosion from tide- or storm-generated rip currents or surges has been also invoked as a cause for the inception and maintenance of shelf-edge conduits (Lewis 1982; Huthnance 1995; Clifton 2006; Normandeau *et al.* 2014), and hyperpycnal flows, wave-supported gravity flows or inertial currents can keep conduits open (Huthnance 1995). These mechanisms cannot be discarded as they can develop local defects that potentially evolve into larger channels as the delta progrades and increases sediment supply, leading to loading and destabilisation of the area (Lewis 1982).

Steeper slopes at the shelf-edge rollover, combined with relatively high sediment loads associated with mouth bar progradation, create conditions for soft-sediment deformation to occur (Owen 2003; Oliveira *et al.* 2011). The amount of soft-sediment deformation (30%), combined with the observed interaction between channels and mixed-influence mouth bar deposits in the middle unit (Fig. 3b) suggest a close association between channel formation and delta-related instabilities (Oliveira *et al.* 2011). Channel incisions are apparently randomly located, but sometimes overlie the axial location of the underlying mixed-influence mouth bar. The local gradient change around the shelf-edge rollover, combined with localised high sediment influx and loading (Wild *et al.* 2009) could have created unstable points around axial positions of mixed-influence mouth bars. Liquefaction and deformation, particularly in their central and thicker parts, were highly susceptible to local remobilisation and gravitational collapse (e.g. Jackson & Johnson 2009), creating discrete bathymetric lows that may have evolved into long-lived conduits through the bypass of gravity flows, generating a highly erosive and channelised shelf-edge rollover.

Accretion and progradation of a shelf-edge rollover

The deformed and sandier parts of lobate elements are generally 5 to 10 m-thick and 80 to 600 m-wide, whereas channels are 5 to 20 m-thick and 50 to 300 m-wide (Fig. 3b and 6). These geometrical proportions are not typical of terminal distributary systems (e.g. Olariu & Bhattacharya 2006; Olariu *et al.* 2010) since delta-related deposits would be expected to be significantly thicker compared to the documented channel dimensions. In the Cretaceous Blackhawk Formation of the Book Cliffs (Utah), prodeltaic channels formed by river-derived hyperpycnal flows are just a few metres thick and encased within mudstone (Pattison 2005; Pattison *et al.* 2007).

In shelf-confined mixed fluvial- and wave-influenced delta systems, feeder channels decrease in size as they reach the lower delta plain, where distributaries split, avulse and decrease in dimensions as they become terminal (Bhattacharya & Giosan 2003; Bhattacharya 2006). Observations made in dip and strike sections at both sides of the Paardeberg Ridge outcrop suggest that when distributary channels reached the shelf-edge rollover, enhanced erosive and bypass processes created larger incisions, and channels became larger and deeper moving downslope across the shelf edge rollover (Figs. 9 and 10). The significant gradient change across the shelf edge rollover may also explain the abrupt facies changes seen in the dip direction. This process might be particularly enhanced when associated with relative sea level fall (Talling 1998; Muto & Steel 2002; Porębski & Steel 2006) and with the proximity of a feeder system (e.g. Mellere *et al.* 2003; Olariu & Bhattacharya 2006). The cross-cutting relationships between channel elements and lobate bodies suggest that the sudden loss of confinement led to deposition of mixed-influence mouth bars that forced distributary channels to step laterally. The smaller channel size up section could reflect the start of backstepping as gradient decreased when approaching the flooding surface above. However, considering that channels are larger and erode more deeply basinward (NE; Fig. 10), the up-section reduction in size within the middle unit is proposed to characterise progradation across the shelf edge rollover (Fig. 11).

Conclusions

The Paardeberg Ridge locality allows the spatial and temporal evolution of a NE prograding shelf margin to be constrained in depositional dip and strike sections. Palaeocurrent data indicate a NW-SE oriented shoreline with dominant NE-SW wave reworking. Truncation of a shallowing upward succession from upper slope turbidites to shelf edge deposits by a 30 m-thick sandstone-rich unit of deformed and mixed-influence mouth bars and subaqueous distributary channels represents an abrupt juxtaposition of paralic deposits on to the shelf edge rollover. The basal erosion surface of the unit is correlated down dip to slope turbidite sandstones, interpreted as deposits of flows that bypassed through the channelised shelf edge rollover. This surface is interpreted as a sequence boundary without subaerial shelf exposure.

In strike section, the older channelised elements are wider, more deeply incised with composite erosion surfaces filled by amalgamated structureless sandstones, and cut into deeper water facies, suggesting recurrent erosion and sediment bypass. Younger channel-fills are narrower with cleaner cuts that incise into shallower water facies, and their fills are better organised with fewer amalgamation surfaces and basal mudstone clast conglomerates, and more beds with symmetrical rippled tops. This is consistent with a vertical change to less erosive and shorter lived channels.

A gradient increase at the shelf-edge, combined with a high rate of sediment supply associated with deltaic progradation promoted soft-sediment deformation. Liquefied mixed-influence mouth bars were susceptible to local remobilisation, and the resulting irregular surfaces likely evolved into subaqueous sediment conduits. When distributaries reached an unstable and relatively steep region, enhanced erosion led to larger and deeper incisions across the shelf edge. The interpreted stratigraphic context and the fact that channels incise into the proximal part of deformed mixed-influence mouth bars suggest that these subaqueous bodies are the shelf-edge expression of distributary channels, associated with an abrupt basinward shift of a mixed-influence deltaic system. This study therefore documents a rare example of the architecture of a progradational mixed-influence paralic succession superimposed on a shelf edge rollover, in response to a lowering of relative sea level.

Acknowledgements

The work presented here is part of the SLOPE Project, Phase 4. We thank the consortium of sponsors (Anadarko, BHPBilliton, BP, CNOOC-Nexen, ConocoPhillips, E.ON, Engie, Maersk, Murphy, Petrobras, Shell, Statoil, Total, VNG Norge and Woodside) for financial support and strong scientific engagement. The manuscript benefited from insightful reviews by Gary Hampson, Cornel Olariu and an anonymous reviewer. Sarah Cobain, Rhodri Jerrett, Eoin Dunlevy and Sascha Eichenauer are thanked for their collaboration and assistance in the field. Finally, we thank the Karoo farmers for access to their land.

References

AINSWORTH, R.B., VAKARELOV, B.K. & NANSON, R.A. 2011. Dynamic spatial and temporal prediction of changes in depositional processes on clastic shorelines: Toward improved subsurface uncertainty reduction and management. *AAPG Bulletin*, **95**, 267-297, doi: 10.1306/06301010036.

Andersson, P.O.D., Worden, R.H., Hodgson, D.M. & Flint, S. 2004. Provenance evolution and chemostratigraphy of a Palaeozoic submarine fan-complex: Tanqua Karoo Basin, South Africa. *Marine and Petroleum Geology*, **21**, 555-577, doi: 10.1016/j.marpetgeo.2004.01.004.

Bhattacharya, J.P. 2006. Deltas. *In*: Walker R.G. & Posamentier H.W. (eds.) *Facies Models revisited, SEPM Special Publication, v. 84*, 237-292.

Bhattacharya, J.P. & Giosan, L. 2003. Wave-influenced deltas: geomorphological implications for facies reconstruction. *Sedimentology*, **50**, 187-210, doi: 10.1046/j.1365-3091.2003.00545.x.

Bhattacharya, J.P. & MacEachern, J.A. 2009. Hyperpycnal rivers and prodeltaic shelves in the Cretaceous seaway of North America. *Journal of Sedimentary Research*, **79**, 184-209.

Bouma, A.H. & Wickens, H.d.V. 1991. Permian passive margin submarine fan complex, Karoo Basin. South Africa: possible model to Gulf of Mexico. *Gulf Coast Association of Geological Societies Transactions*, **41**, 30-42.

Bourget, J., Ainsworth, R.B. & Thompson, S. 2014. Seismic stratigraphy and geomorphology of a tide or wave dominated shelf-edge delta (NW Australia): Process-based classification from 3D seismic attributes and implications for the prediction of deep-water sands. *Marine and Petroleum Geology*, **57**, 359-384, doi: http://dx.doi.org/10.1016/j.marpetgeo.2014.05.021.

Bowman, A.P. & Johnson, H.D. 2014. Storm-dominated shelf-edge delta successions in a high accommodation setting: The palaeo-Orinoco Delta (Mayaro Formation), Columbus Basin, South-East Trinidad. *Sedimentology*, **61**, 792-835, doi: 10.1111/sed.12080.

Carvajal, C.R. & Steel, R.J. 2006. Thick turbidite successions from supply-dominated shelves during sea-level highstand. *Geology*, **34**, 665-668, doi: 10.1130/g22505.1.

Carvajal, C. & Steel, R. 2009. Shelf-edge architecture and bypass of sand to deep water: influence of shelf-edge processes, sea level, and sediment supply. *Journal of Sedimentary Research*, **79**, 652-672, doi: 10.2110/jsr.2009.074.

Cattaneo, A., Trincardi, F., Asioli, A. & Correggiari, A. 2007. The Western Adriatic shelf clinoform: energy-limited bottomset. *Continental Shelf Research*, **27**, 506-525.

Catuneanu, O., Hancox, P.J. & Rubidge, B.S. 1998. Reciprocal flexural behaviour and contrasting stratigraphies: a new basin development model for the Karoo retroarc foreland system, South Africa. *Basin Research*, **10**, 417-439, doi: 10.1046/j.1365-2117.1998.00078.x.

Clifton, H.E. 2006. A re-examination of facies models for clastic shorelines. *In*: Posamentier, H.W. & Walker, R.G. (eds.) *Facies Models Revisited, SEPM Special Publications, vol. 84* 293-337.

Cole, D.I. 1992. Evolution and development of the Karoo Basin. *In*: de Wit, M.J. & Ransome, I.G.D. (eds.) *Inversion Tectonics of the Cape Fold Belt, Karoo and Cretaceous Basins of Southern Africa*, A.A. Balkema, Rotterdam, 87-99.

Covault, J.A., Romans, B.W. & Graham, S.A. 2009. Outcrop Expression of a Continental-Margin-Scale Shelf-Edge Delta from the Cretaceous Magallanes Basin, Chile. *Journal of Sedimentary Research*, **79**, 523-539, doi: 10.2110/jsr.2009.053.

Crumeyrolle, P., Renaud, I. & Suiter, J. 2007. The use of two- and three-dimensional seismic to understand sediment transfer from fluvial to deepwater via sinuous channels: example from the Mahakam shelf and comparison with outcrop data (south central Pyrenees). *Geological Society, London, Special Publications*, **277**, 85-103, doi: 10.1144/gsl.sp.2007.277.01.05.

De Beer, C.H. 1992. Structural evolution of the Cape Fold Belt syntaxis and its influence on syntectonic sedimentation in the SW Karoo Basin. *In*: de Wit, M.J. & Ransome, I.G.D. (eds.) *Inversion Tectonics of the Cape Fold Belt, Karoo and Cretaceous Basins of Southern Africa*, A.A. Balkema, Rotterdam, 197-206.

Dixon, J.F., Steel, R.J. & Olariu, C. 2012a. River-dominated, shelf-edge deltas: delivery of sand across the shelf break in the absence of slope incision. *Sedimentology*, **59**, 1133-1157, doi: 10.1111/j.1365-3091.2011.01298.x.

Dixon, J.F., Steel, R.J. & Olariu, C. 2012b. Shelf-edge delta regime as a predictor of deep-water deposition. *Journal of Sedimentary Research*, **82**, 681-687, doi: 10.2110/jsr.2012.59.

Donovan, A.D. 2003. Depositional topography and sequence development. . *In*: Roberts, H.H., Rosen, N.C., Fillon, R.H. & Anderson, J.B. (eds.) *Shelf Margin Deltas and linked Down Slope Petroleum Systems: Global Significance and Future Exploration Potential*, GCSSEPM Foundation 23rd Annual Bob F. Perkins Research Conference, 493-522.

Edwards, M.B. 1981. Upper Wilcox Rosita delta system of South Texas; growth-faulted shelf-edge deltas. *AAPG Bulletin*, **65**, 54-73.

Faure, K. & Cole, D. 1999. Geochemical evidence for lacustrine microbial blooms in the vast Permian Main Karoo, Parana, Falkland Islands and Huab basins of southwestern Gondwana. *Palaeogeography, Palaeoclimatology, Palaeoecology*, **152**, 189-213.

FLINT, S. S., HODGSON, D. M., SPRAGUE, A. R., BRUNT, R. L., VAN DER MERWE, W. C., FIGUEIREDO, J., PRELAT, A., BOX, D., DI CELMA, C & KAVANAGH, J. P. 2011. Depositional architecture and sequence stratigraphy of the Karoo basin floor to shelf edge succession, Laingsburg depocentre, South Africa. *Marine and Petroleum Geology*, **28**(3), 658-674.

FULTHORPE, C.S. & AUSTIN, J.A. 1998. Anatomy of rapid margin progradation; three-dimensional geometries of Miocene clinoforms, New Jersey margin. *AAPG Bulletin*, **82**, 251-273.

FULTHORPE, C.S., AUSTIN, J.A. & MOUNTAIN, G.S. 1999. Buried fluvial channels off New Jersey: Did sea-level lowstands expose the entire shelf during the Miocene? *Geology*, **27**, 203-206, doi: 10.1130/0091-7613(1999)027<0203:bfconj>2.3.co;2.

FULTHORPE, C.S., AUSTIN, J.A. & MOUNTAIN, G.S. 2000. Morphology and distribution of Miocene slope incisions off New Jersey: Are they diagnostic of sequence boundaries? *Geological Society of America Bulletin*, **112**, 817-828, doi: 10.1130/0016-7606(2000)112<817:madoms>2.0.co;2.

GALLOWAY, W.E. 1998. Siliciclastic slope and base-of-slope depositional systems; component facies, stratigraphic architecture, and classification. *AAPG Bulletin*, **82**, 569-595.

HADLER-JACOBSEN, F., JOHANNESSEN, E.P., ASHTON, N., HENRIKSEN, S., JOHNSON, S.D. & KRISTENSEN, J.B. 2005. Submarine fan morphology and lithology distribution: a predictable function of sediment delivery, gross shelf-to-basin relief, slope gradient and basin relief/topography. *In*: DORÉ, A.G. & VINING, B.A. (eds.) *Petroleum Geology: North West Europe and Global Perspectives, Proceedings of the 6th Petroleum Geology Conference, London (UK)*, 1121-1145.

HAMPSON, G.J. 2000. Discontinuity Surfaces, Clinoforms, and Facies Architecture in a Wave-Dominated, Shoreface-Shelf Parasequence. *Journal of Sedimentary Research*, **70**, 325-340, doi: 10.1306/2dc40914-0e47-11d7-8643000102c1865d.

HAMPSON, G.J. & HOWELL, J.A. 2005. Sedimentologic and geomorphic characterization of ancient wave-dominated deltaic shorelines; Upper Cretaceous Blackhawk Formation, Book Cliffs, Utah, U.S.A. *In*: GIOSAN, L. & BHATTACHARHYA, J.P. (eds.) *River Deltas – Concepts, Models, and Examples. SEPM Special Publication 83*, 133-154.

HELLAND-HANSEN, W. 2010. Facies and stacking patterns of shelf-deltas within the Palaeogene Battfjellet Formation, Nordenskiöld Land, Svalbard: implications for subsurface reservoir prediction. *Sedimentology*, **57**, 190-208, doi: 10.1111/j.1365-3091.2009.01102.x.

Henriksen, S., Helland-Hansen, W. & Bullimore, S. 2011. Relationships between shelf-edge trajectories and sediment dispersal along depositional dip and strike: a different approach to sequence stratigraphy. *Basin Research*, **23**, 3-21, doi: 10.1111/j.1365-2117.2010.00463.x.

Hodgson, D.M., Flint, S.S., Hodgetts, D., Drinkwater, N.J., Johannessen, E.P. & Luthi, S.M. 2006. Stratigraphic Evolution of Fine-Grained Submarine Fan Systems, Tanqua Depocenter, Karoo Basin, South Africa. *Journal of Sedimentary Research*, **76**, 20-40, doi: 10.2110/jsr.2006.03.

Hubbard, S.M., Fildani, A., Romans, B.W., Covault, J.A. & McHargue, T.R. 2010. High-relief slope clinoform development: Insights from outcrop, Magallanes Basin, Chile. *Journal of Sedimentary Research*, **80**, 357-375, doi: 10.2110/jsr.2010.042.

Huthnance, J.M. 1995. Circulation, exchange and water masses at the ocean margin: the role of physical processes at the shelf edge. *Progress in Oceanography*, **35**, 353-431, doi: http://dx.doi.org/10.1016/0079-6611(95)80003-C.

Ivanov, V.V., Shapiro, G.I., Huthnance, J.M., Aleynik, D.L. & Golovin, P.N. 2004. Cascades of dense water around the world ocean. *Progress in Oceanography*, **60**, 47-98, doi: http://dx.doi.org/10.1016/j.pocean.2003.12.002.

Jackson, C.A.L. & Johnson, H.D. 2009. Sustained turbidity currents and their interaction with debrite-related topography; Labuan Island, offshore NW Borneo, Malaysia. *Sedimentary Geology*, **219**, 77-96, doi: http://dx.doi.org/10.1016/j.sedgeo.2009.04.008.

Johnson, M.R. 1991. Sandstone petrography, provenance and plate tectonic setting in Gondwana context of the southeastern Cape-Karoo Basin. *South African Journal of Geology*, **94**, 137-154.

Johnson, M.R., van Vuuren, C.J., Visser, J.N.J., Cole, D.I., Wickens, H.d.V., Christie, A.D.M., Roberts, D.L. & Brandl, G. 2006. Sedimentary rocks of the Karoo Supergroup. *In*: Johnson, M.R., Anhaeusser, C.R. & Thomas, R.J. (eds.) *The geology of South Africa*, Geological Society of South Africa and Council for Geoscience, Pretoria, 461-499.

Johnson, S.D., Flint, S., Hinds, D. & De Ville Wickens, H. 2001. Anatomy, geometry and sequence stratigraphy of basin floor to slope turbidite systems, Tanqua Karoo, South Africa. *Sedimentology*, **48**, 987-1023.

Jones, G.E.D., Hodgson, D.M. & Flint, S.S. 2013. Contrast in the process response of stacked clinothems to the shelf-slope rollover. *Geosphere*, **9**, 299-316, doi: 10.1130/ges00796.1.

JONES, G.E.D., HODGSON, D.M. & FLINT, S.S. 2015. Lateral variability in clinoform trajectory, process regime, and sediment dispersal patterns beyond the shelf-edge rollover in exhumed basin margin-scale clinothems. *Basin Research*, **27**, 657-680.

KOLLA, V., BIONDI, P., LONG, B. & FILLON, R. 2000. Sequence stratigraphy and architecture of the Late Pleistocene Lagniappe delta complex, northeast Gulf of Mexico. *Geological Society, London, Special Publications*, **172**, 291-327, doi: 10.1144/gsl.sp.2000.172.01.14.

LEWIS, D.W. 1982. Channels across continental shelves: Corequisites of canyon-fan systems and potential petroleum conduits. *New Zealand Journal of Geology and Geophysics*, **25**, 209-225, doi: 10.1080/00288306.1982.10421410.

LUTHI, S.M., HODGSON, D.M., GEEL, C.R., FLINT, S.S., GOEDBLOED, J.W., DRINKWATER, N.J. & JOHANESSEN, E.P. 2006. Contribution of research borehole data to modelling fine-grained turbidite reservoir analogues, Permian Tanqua-Karoo basin floor fans (South Africa). *Petroleum Geology*, **12**, 175-190.

MACQUAKER, J.H.S. & BOHACS, K.M. 2007. On the Accumulation of Mud. *Science*, **318**, 1734-1735, doi: 10.1126/science.1151980.

MATTEUCCI, T.D. & HINE, A.C. 1987. Evolution of the Cape Fear Terrace: A complex interaction between the Gulf Stream and a paleo-shelf edge delta. *Marine Geology*, **77**, 185-205, doi: http://dx.doi.org/10.1016/0025-3227(87)90111-3.

MAYALL, M.J., YEILDING, C.A., OLDROYD, J.D., PULHAM, A.J. & SAKURAI, S. 1992. Facies in a shelf-edge delta; an example from the subsurface of the Gulf of Mexico, middle Pliocene, Mississippi Canyon, Block 109. *AAPG Bulletin*, **76**, 435-448.

MAZIÈRES, A., GILLET, H., CASTELLE, B., GUYOT, C., MULDER, T. & MALLET, C. 2013. Relationship between longshore drift and the head of the canyon of Capbreton (SW France): descriptive and numerical approaches. *Proceedings of the 7th International Conference on Coastal Dynamics*, 24-28 June, Arcachon, France, 1159-1172.

MELLERE, D., BREDA, A. & STEEL, R.J. 2003. Fluvial-incised shelf-edge deltas and linkage to upper-slope channels (Central Tertiary Basin, Spitsbergen). *Shelf-Margin Deltas and Linked Downslope Petroleum Systems: Global Significance and Future Exploration Potential, Gulf Coast Section. 23rd Annual Research Conference Houston, Texas*, 231-266.

Mellere, D., Plink-Björklund, P. & Steel, R.J. 2002. Anatomy of shelf deltas at the edge of a prograding Eocene shelf margin, Spitsbergen. *Sedimentology*, **49**, 1181-1206.

Milton, N. & Dyce, M. 1995. Systems tract geometries associated with Early Eocene lowstands, imaged on a 3D seismic dataset from the Bruce area, UK North Sea. *in Steel, R. J.; Felt, V. L.; Johannessen, E. P.; and Mathieu, C., eds. Sequence stratigraphy on the northwest European margin. Norwegian Petroleum Society, Special Publication no. 5*, 429-449.

Morton, R.A. & Suter, J.R. 1996. Sequence Stratigraphy and Composition of Late Quaternary Shelf-Margin Deltas, Northern Gulf of Mexico. *AAPG Bulletin*, **80**, 505-530.

Moscardelli, L., Wood, L.J. & Dunlap, D.B. 2012. Shelf-edge deltas along structurally complex margins: A case study from eastern offshore Trinidad. *AAPG Bulletin*, **96**, 1483-1522, doi: 10.1306/01241211046.

Mulder, T., Syvitski, J.P.M., Migeon, S., Faugères, J.C. & Savoye B. 2003. Hyperpycnal turbidity currents: initiation, behavior and related deposits: a review. *Marine and Petroleum Geology 20*, 861-882.

Muto, T. & Steel, R.J. 2002. In Defense of Shelf Edge Delta Development during Falling and Lowstand of Relative Sea Level. *The Journal of Geology*, **110**, 421-436, doi: 10.1086/340631.

Mutti, E., Tinterri, R., Benevelli, G., DiBiase, D. & Cavanna, G. 2003. Deltaic, mixed and turbidite sedimentation of ancient foreland basins. *Turbidites: Models and Problems (Eds E. Mutti, G.S. Steffens, C. Pirmez, M. Orlando and D. Roberts), Marine and Petroleum Geology*, **20**, 733-755.

Normandeau, A., Lajeunesse, P., St-Onge, G., Bourgault, D., Drouin, S.S.-O., Senneville, S. & Belanger, S. 2014. Morphodynamics in sediment-starved inner-shelf submarine canyons (Lower St. Lawrence Estuary, Eastern Canada). *Marine Geology*, **357**, 243-255, doi: http://dx.doi.org/10.1016/j.margeo.2014.08.012.

Nøttvedt, A. & Kreisa, R.D. 1987. Model for the combined-flow origin of hummocky cross-stratification. 357-361.

Olariu, C. 2014. Autogenic process change in modern deltas. *From Depositional Systems to Sedimentary Successions on the Norwegian Continental Margin*. John Wiley & Sons, Ltd, 149-166.

Olariu, C. & Bhattacharya, J.P. 2006. Terminal distributary channels and delta front architecture of river-dominated delta systems. *Journal of Sedimentary Research*, **76**, 212-233, doi: 10.2110/jsr.2006.026.

OLARIU, C. & STEEL, R.J. 2009. Influence of point-source sediment-supply on modern shelf-slope morphology: implications for interpretation of ancient shelf margins. *Basin Research*, **21**, 484-501, doi: 10.1111/j.1365-2117.2009.00420.x.

OLARIU, C., STEEL, R.J. & PETTER, A.L. 2010. Delta-front hyperpycnal bed geometry and implications for reservoir modeling: Cretaceous Panther Tongue delta, Book Cliffs, Utah. *AAPG Bulletin*, **94**, 819-845.

OLARIU, M.I., CARVAJAL, C.R., OLARIU, C. & STEEL, R.J. 2012. Deltaic process and architectural evolution during cross-shelf transits, Maastrichtian Fox Hills Formation, Washakie Basin, Wyoming. *AAPG Bulletin*, **96**, 1931-1956.

OLIVEIRA, C.M.M., HODGSON, D.M. & FLINT, S.S. 2011. Distribution of soft-sediment deformation structures in clinoform successions of the Permian Ecca Group, Karoo Basin, South Africa. *Sedimentary Geology*, **235**, 314-330.

OWEN, G. 2003. Load structures: gravity-driven sediment mobilization in the shallow subsurface. *Geological Society, London, Special Publications*, **216**, 21-34, doi: 10.1144/gsl.sp.2003.216.01.03.

PATRUNO, S., HAMPSON, G.J. & JACKSON, C.A.L. 2015. Quantitative characterisation of deltaic and subaqueous clinoforms. *Earth-Science Reviews*, **142**, 79-119, doi: http://dx.doi.org/10.1016/j.earscirev.2015.01.004.

PATTISON, S.A. 2005. Storm-influenced prodelta turbidite complex in the Lower Kenilworth Member at Hatch Mesa, Book Cliffs, Utah, USA: implications for shallow marine facies models. *Journal of Sedimentary Research*, **75**, 420-439.

PATTISON, S.A., BRUCE AINSWORTH, R. & HOFFMAN, T.A. 2007. Evidence of across-shelf transport of fine-grained sediments: turbidite-filled shelf channels in the Campanian Aberdeen Member, Book Cliffs, Utah, USA. *Sedimentology*, **54**, 1033-1064.

PETTER, A.L. & STEEL, R.J. 2005. Deepwater-slope channels and hyperpycnal flows from the Eocene of the central Spitsbergen Basin: Predicting basin-floor sands from a shelf edge/upper slope perspective. *AAPG Annual Meeting, June 19–22, 2005, Calgary, Alberta*.

PETTER, A.L. & STEEL, R.J. 2006. Hyperpycnal flow variability and slope organization on an Eocene shelf margin, Central Basin, Spitsbergen. *AAPG Bulletin*, **90**, 1451-1472.

Pirmez, C., Pratson, L.F. & Steckler, M.S. 1998. Clinoform development by advection-diffusion of suspended sediment: Modeling and comparison to natural systems. *Journal of Geophysical Research*, **103**, 24141-24157, doi: 10.1029/98jb01516.

Plink-Björklund, P. & Steel, R. 2002. Sea-level fall below the shelf edge, without basin-floor fans. *Geology*, **30**, 115-118.

Plink-Björklund, P. & Steel, R.J. 2004. Initiation of turbidity currents: Outcrop evidence for Eocene hyperpycnal flow turbidites. *Sedimentary Geology*, **165**, 29-52.

Plink-Björklund, P. & Steel, R. 2005. Deltas on falling-stage and lowstand shelf margins, the Eocene Central Basin of Spitsbergen: importance of sediment supply. *In*: Giosan, L. & Bhattacharya, J.P. (eds.) *River Deltas - Concepts, Models, and Examples, SEPM, Special Publication 83*, 179-206.

Poag, C.W., Swift, B.A., Schlee, J.S., Ball, M.M. & Sheetz, L.L. 1990. Early Cretaceous shelf-edge deltas of the Baltimore Canyon Trough: Principal sources for sediment gravity deposits of the northern Hatteras Basin. *Geology*, **18**, 149-152, doi: 10.1130/0091-7613(1990)018<0149:ecsedo>2.3.co;2.

Pontén, A. & Plink-Björklund, P. 2009. Process Regime Changes Across a Regressive to Transgressive Turnaround in a Shelf–Slope Basin, Eocene Central Basin of Spitsbergen. *Journal of Sedimentary Research*, **79**, 2-23, doi: 10.2110/jsr.2009.005.

Porębski, S.J. & Steel, R.J. 2003. Shelf-margin deltas: their stratigraphic significance and relation to deepwater sands. *Earth-Science Reviews*, **62**, 283-326.

Porębski, S.J. & Steel, R.J. 2006. Deltas and sea-level change. *Journal of Sedimentary Research*, **76**, 390-403.

Posamentier, H.W., Jervey, M.T. & Vail, P.R. 1988. Eustatic controls on clastic deposition I - conceptual framework. *in C.K. Wilgus, B.S. Hastings, C.G.S.C. Kendall, H.W. Posamentier, C.A. Ross and J.C. Van Wagoner eds., Sea Level Changes - An Integrated Approach, SEPM Special Publication*, **42**.

Posamentier, H.W. & Kolla, V. 2003. Seismic Geomorphology and Stratigraphy of Depositional Elements in Deep-Water Settings. *Journal of Sedimentary Research*, **73**, 367-388, doi: 10.1306/111302730367.

Pratson, L.F., Ryan, W.B.F., Mountain, G.S. & Twichell, D.C. 1994. Submarine canyon initiation by downslope-eroding sediment flows: Evidence in late Cenozoic strata on the New Jersey continental slope. *Geological Society of America Bulletin*, **106**, 395-412, doi: 10.1130/0016-7606(1994)106<0395:scibde>2.3.co;2.

Prélat, A., Pankhania Shyam, S., Jackson, C., A-L. & Hodgson, D.M. 2015. Slope gradient and lithology as controls on the initiation of submarine slope gullies; insights from the North Carnarvon Basin, Offshore NW Australia. *Sedimentary Geology*, doi: http://dx.doi.org/10.1016/j.sedgeo.2015.08.009.

Pyles, D.R. & Slatt, R.M. 2000. A high-frequency sequence stratigraphic framework for the shallow through deep-water deposits of the Lewis Shale and Fox Hills Sandstone, Great Divide and Washakie basins, Wyoming. *In*: Weimer, P., Slatt, R.M., Coleman, J., Rosen, N.C., Nelson, C.H., Bouma, A.H., Styzen, M.J. & Lawrence, D.T. (eds.) *Deep-Water Reservoirs of the World, SEPM, Gulf Coast Section, 20th Annual Research Conference, Houston, Texas*, 836-861.

Pyles, D.R. & Slatt, R.M. 2007. Applications to understanding shelf edge to base-of-slope changes in stratigraphic architecture of prograding basin margins: Stratigraphy of the Lewis Shale, Wyoming, USA. *In*: Nilsen, T.H., Shew, R.D., Steffens, G.S. & Studlick, J.R.J. (eds.) *Atlas of Deepwater Outcrops: AAPG Studies in Geology 56*, 485-489.

Ridente, D., Foglini, F., Minisini, D., Trincardi, F. & Verdicchio, G. 2007. Shelf-edge erosion, sediment failure and inception of Bari Canyon on the Southwestern Adriatic Margin (Central Mediterranean). *Marine Geology*, **246**, 193-207, doi: http://dx.doi.org/10.1016/j.margeo.2007.01.014.

Ross, W.C., Halliwell, B.A., May, J.A., Watts, D.E. & Syvitski, J.P.M. 1994. Slope readjustment: a new model for the development of submarine fans and aprons. *Geology*, **22**, 511-514.

Rubin, D.M. & McCulloch, D.S. 1980. Single and superimposed bedforms: a synthesis of San Francisco Bay and flume observations. *Sedimentary Geology*, **26**, 207-231.

Ryan, M.C., Helland-Hansen, W., Johannessen, E.P. & Steel, R.J. 2009. Erosional vs. accretionary shelf margins: the influence of margin type on deepwater sedimentation: an example from the Porcupine Basin, offshore western Ireland. *Basin Research*, **21**, 676-703, doi: 10.1111/j.1365-2117.2009.00424.x.

Saller, A.H., Noah, J.T., Ruzuar, A.P. & Schneider, R. 2004. Linked lowstand delta to basin-floor fan deposition, offshore Indonesia: An analog for deep-water reservoir systems. *AAPG Bulletin*, **88**, 21-46, doi: 10.1306/09030303003.

Sanchez, C.M., Fulthorpe, C.S. & Steel, R.J. 2012a. Middle Miocene–Pliocene siliciclastic influx across a carbonate shelf and influence of deltaic sedimentation on shelf construction, Northern Carnarvon Basin, Northwest Shelf of Australia. *Basin Research*, **24**, 664-682, doi: 10.1111/j.1365-2117.2012.00546.x.

Sanchez, C.M., Fulthorpe, C.S. & Steel, R.J. 2012b. Miocene shelf-edge deltas and their impact on deepwater slope progradation and morphology, Northwest Shelf of Australia. *Basin Research*, **24**, 683-698, doi: 10.1111/j.1365-2117.2012.00545.x.

Schieber, J., Southard, J. & Thaisen, K. 2007. Accretion of Mudstone Beds from Migrating Floccule Ripples. *Science*, **318**, 1760-1763, doi: 10.1126/science.1147001.

Scott, E.D., Bouma, A.H. & Wickens, H.d.V. 2000. Influence of tectonics on submarine fan deposition, Tanqua and Laingsburg subbasins, South Africa. *In*: A.H., B. & Stone, C.G. (eds.) *Fine-grained turbidite systems, American Association of Petroleum Geologists Memoir 72*, 47-56.

Shapiro, G.I. & Hill, A.E. 1997. Dynamics of Dense Water Cascades at the Shelf Edge. *Journal of Physical Oceanography*, **27**, 2381-2394, doi: 10.1175/1520-0485(1997)027<2381:dodwca>2.0.co;2.

Smith, R.M.H. 1990. A review of stratigraphy and sedimentary environments of the Karoo Basin of South Africa. *Journal of African Earth Sciences (and the Middle East)*, **10**, 117-137, doi: http://dx.doi.org/10.1016/0899-5362(90)90050-O.

Southard, J.B. 1971. Representation of bed configurations in depth-velocity-size diagrams. *Journal of Sedimentary Petrology*, **41**, 903-915.

Southard, J.B. & Boguchwal, L.A. 1990. Bed configurations in steady unidirectional water flows. Part 2. Synthesis of flume data. *Journal of Sedimentary Research*, **60**, 658-679.

Southard, J.B., Lambie, J.M., Federico, D.C., Pile, H.T. & Weidman, C.R. 1990. Experiments on bed configurations in fine sands under bidirectional purely oscillatory flow, and the origin of hummocky cross-stratification. *Journal of Sedimentary Research*, **60**, 1-17, doi: 10.1306/212f90f7-2b24-11d7-8648000102c1865d.

Stear, W.M. 1983. Morphological characteristics of ephemeral stream channel and overbanks splay sandstone bodies in the Permian Lower Beaufort Group, Karoo Basin, South Africa. *In*: Collinson, J.D. & Lewin, J. (eds.) *Modern and Ancient Fluvial Systems: International Association of Sedimentologists, Special Publication 6*, 405-420.

Stear, W.M. 1985. Comparison of the bedform distribution and dynamics of modern and ancient sandy ephemeral flood deposits in the southwestern Karoo region, South Africa. *Sedimentary Geology*, **45**, 209-230.

Steel, R.J., Crabaugh, J., Schelpepper, M., Mellere, D., Plink-Björklund, P., Deibert, J. & Løseth, T. 2000. Deltas vs. rivers on the shelf edge: their relative contributions to the growth of shelf-margins and basin-floor fans (Barremian and Eocene, Spitsbergen). *GCSSEPM Foundation 20th Annual Bob F. Perkins Research Conference*, 981–1009.

Steel, R.J., Porebski, S.J., Plink-Bjorklund, P., Mellere, D. & Schellpeper, M. 2003. Shelf-edge delta types and their sequence-stratigraphic relationships. *Shelf Margin Deltas and Linked Down Slope Petroleum Systems: Global Significance and Future Exploration Potential*, Houston, Texas. December 7-10., 205-230.

Stevenson, C.J., Jackson, C.A.-L., Hodgson, D.M., Hubbard, S.M. & Eggenhuisen, J.T. 2015. Deep-water sediment bypass. *Journal of Sedimentary Research*, **85**, 1058-1081.

Suter, J.R. & Berryhill, H.L. 1985. Late Quaternary shelf-margin deltas, Northwest Gulf of Mexico. *AAPG Bulletin*, **69**, 77-91.

Sydow, J. & Roberts, H.H. 1994. Stratigraphic framework of a late Pleistocene shelf-edge delta, Northeast Gulf of Mexico. *AAPG Bulletin*, **78**, 1276-1312.

Sylvester, Z., Deptuck, M.E., Prather, B.E., Pirmez, C. & O'Byrne, C. 2012. Seismic Stratigraphy of a Shelf-Edge Delta and Linked Submarine Channels in the Northeastern Gulf of Mexico. *In*: Prather, B., Deptuck, M.E., Mohrig, D., Van Hoor, B. & Wynn, R.B. (eds.) *Application of the Principles of Seismic Geomorphology to Continental-Slope and Base-of-Slope Systems: Case Studies from Seafloor and Near-Seafloor Analogues, SEPM Society for Sedimentary Geology Special Publication, 99*, 31-59.

Talling, P.J. 1998. How and where do incised valleys form if sea level remains above the shelf edge? *Geology*, **26**, 87-90, doi: 10.1130/0091-7613(1998)026<0087:hawdiv>2.3.co;2.

Tankard, A., Welsink, H., Aukes, P., Newton, R. & Stettler, E. 2009. Tectonic evolution of the Cape and Karoo basins of South Africa. *Marine and Petroleum Geology*, **26**, 1379-1412, doi: 10.1016/j.marpetgeo.2009.01.022.

Tesson, M., Gensous, B., Allen, G.P. & Ravenne, C. 1990. Late Quaternary deltaic lowstand wedges on the Rhône continental shelf, France. *Marine Geology*, **91**, 325-332, doi: http://dx.doi.org/10.1016/0025-3227(90)90053-M.

Tinterri, R. 2007. The lower Eocene Roda Sandstone (South-Central Pyrenees): an example of a flood-dominated river-delta system in a tectonically controlled basin. *Rivista Italiana di Paleontologia e Stratigrafia*, **113**, 223-255.

Turner, B.R. 1981. Possible origin of low angle cross-strata and horizontal lamination in Beaufort Group sandstones of the southern Karoo Basin. *Geological Society of South Africa, Transactions*, **84**, 193-197.

Turner, B.R. 1999. Tectonostratigraphical development of the Upper Karoo foreland basin: Orogenic unloading versus thermally-induced Gondwana rifting. *Journal of African Earth Sciences*, **28**, 215-238.

Uroza, C.A. & Steel, R.J. 2008. A highstand shelf-margin delta system from the Eocene of West Spitsbergen, Norway. *Sedimentary Geology*, **203**, 229-245.

Van den Berg, J.H. & Van Gelder, A. 1993. A new bedform stability diagram, with emphasis on the transition of ripples to plane bed in flows over fine sand and silt. *In*: Marzo, M. & Puigdefabregas, C. (eds.) *Alluvial Sedimentation, International Association of Sedimentologists, Special Publication 17*, 11-21.

van der Werff, W. & Johnson, S. 2003. High resolution stratigraphic analysis of a turbidite system, Tanqua Karoo Basin, South Africa. *Marine and Petroleum Geology*, **20**, 45-69, doi: http://dx.doi.org/10.1016/S0264-8172(03)00025-4.

Van Wagoner, J.C., Mitchum, R.M., Campion, K.M. & Rahmanian, V.D. 1990. Siliciclastic sequence stratigraphy in well logs, cores, and outcrops. American Association of Petroleum Geologists Methods in Exploration Series, No. 7, Tulsa, Oklahoma.

Veevers, J.J., Cole, D.I. & Cowan, E.J. 1994. Southern Africa: Karoo Basin and Cape Fold Belt. *In*: Veevers, J.J. & Powell, C.M. (eds.) *Permian-Triassic Pangean basins and foldbelts along the Panthalassan Margin of Gondwanaland. Geological Society America Memoir 184*, 223-279.

VIANA, A.R., HERCOS, C.M., DE ALMEIDA, W., MAGALHÃES, J.L. & DE ANDRADE, S.B. 2002. Evidence of bottom current influence on the Neogene to Quaternary sedimentation along the northern Campos Slope, SW Atlantic Margin. *In*: STOW, D.A.V., FAUGÈRES, J.-C., PUDSEY, C.J., HOWE, J.A. & VIANA, A.R. (eds.) *Deep-Water Contourite Systems: Modern Drifts and Ancient Series, Seismic and Sedimentary Characteristics. Geological Society, London, Memoir 22*, 249-259.

VISSER, J.N.J. 1993. Sea-level changes in a back-arc-foreland transition: the late Carboniferous-Permian Karoo Basin of South Africa. *Sedimentary Geology*, **83**, 115-131, doi: http://dx.doi.org/10.1016/0037-0738(93)90185-8.

WICKENS, H.D.V. 1994. Basin Floor Fan Building Turbidites of the Southwestern Karoo Basin, Permian Ecca Group, South Africa. [unpublished Ph.D. Thesis]. *University of Port Elizabeth, Port Elizabeth (South Africa)*, 233.

WILD, R. 2005. *Sedimentological and sequence stratigraphic evolution of a Permian lower slope to shelf succession, Tanqua depocentre, SW Karoo Basin, South Africa. PhD Thesis*, University of Liverpool.

WILD, R., FLINT, S.S. & HODGSON, D.M. 2009. Stratigraphic evolution of the upper slope and shelf edge in the Karoo Basin, South Africa. *Basin Research*, **21**, 502-527.

WILD, R., HODGSON, D.M. & FLINT, S.S. 2005. Architecture and stratigraphic evolution of multiple, vertically-stacked slope channel complexes, Tanqua depocentre, Karoo Basin, South Africa. *In*: HODGSON, D.M. & FLINT, S.S. (eds.) *Submarine Slope Systems: Processes and Products. Geological Society of London Special Publication 244*, 89-111.

WILSON, A., FLINT, S., PAYENBERG, T., TOHVER, E. & LANCI, L. 2014. Architectural Styles and Sedimentology of the Fluvial Lower Beaufort Group, Karoo Basin, South Africa. *Journal of Sedimentary Research*, **84**, 326-348, doi: 10.2110/jsr.2014.28.

WILSON, P.A. & ROBERTS, H.H. 1995. Density cascading: off-shelf sediment transport, evidence and implications, Bahama Banks. *Journal of Sedimentary Research*, **65**, 45-56, doi: 10.1306/d426801d-2b26-11d7-8648000102c1865d.

ZAVALA, C., ARCURI, M., DI MEGLIO, M., GAMERO, H. & CONTRERAS, C. 2011. A genetic facies tract for the analysis of sustained hyperpycnal flow deposits. *In*: SLATT, R.M. & ZAVALA, C. (eds.) *Sediment transfer from shelf to deep water - Revisiting the delivery system. AAPG Studies in Geology 61*, 1-21.

Figure captions

Fig. 1: (a) The southwestern Karoo Basin with Tanqua and Laingsburg depocentres outlined. (b) The Tanqua depocentre study area. (c) Detailed map of the Paardeberg Ridge locality. Log positions are shown in white, and black lines indicate mapped erosion surfaces. Images from Google Earth.

Fig. 2: (a) Summary stratigraphy of the Tanqua Depocentre adapted from Wickens (1994), Wild *et al.* (2009) and Flint *et al.* (2011). The Waterford Formation here includes the Kookfontein Formation. (b) Summary log (DRs in Fig.1c) of the Paardeberg Ridge succession. The middle unit is the focus of this work

Fig. 3: (a) Vertically exaggerated photo-panorama of the SW face of the Paardeberg Ridge. Log positions are shown in white. (b) Architectural detail of the middle unit. Black lines mark the contacts between different elements and red dotted lines show the positions of mudstone clast lags. All depositional elements have been coded, for example t1C or t4L, where “t1” or “t4” is related to the relative time of deposition, inferred from the lateral and vertical relationships between the elements. “C” or “L” refers to channelised or lobate body. The oldest erosion surface ($t1_C$) that truncates distal prodelta facies of the uppermost slope parasequences is interpreted as the basal sequence boundary of the middle unit.

Fig. 4: Rose diagrams showing palaeocurrent distribution for the (a) lower, middle and upper units; and comparing (b) channelised vs. (c) lobate bodies, showing measurements within the different parts of the elements; (d) types of measurements. Dark colour represents bidirectional measurements while light colour represents unidirectional measurements. Def = deformation.

Fig. 5: Representative photographs of lithofacies from the middle unit. Table 1 outlines the lithofacies codes and interpretation of depositional processes (Ci: Matrix- to clast-supported intraformational

conglomerate; Cm: Mudstone clast horizon; Ss: Structureless sandstone; Sr: Ripple or climbing ripple-lamination; Sg: Inverse to normal graded sandstone; Sp: Parallel bedded sandstone; Sx: High angle planar or trough-cross bedded sandstone Sw: wavy lamination and symmetrical ripple-lamination).

Fig. 6: Dimensions, geometries and facies associations observed by depositional element, for channelised bodies (symmetric, asymmetric or amalgamated fills) and lobate bodies. Sd: Sandstone; St: Siltstone. Below: Summary table of width, thickness and length (">" maximum measured due to outcrop constrains) values for the channelised and lobate elements measured in the Paardeberg ridge.

Fig. 7: Map of the channelised elements from SW to NE of the Paardeberg Ridge. Black lines represent mapped erosion surfaces. Dotted lines represent correlative surfaces between the two sides of the Paardeberg Ridge. Arrows represent main palaeocurrents. Right hand side table summarise the differences observed comparing the elements in up dip and down dip positions.

Fig. 8: Idealised geometrical relationships observed between channelised and lobate elements in strike section. Colour code is the same as in Figures 3 and 6. Left log shows a lobe element cut by a channelised element and overlain by the off-axis part of another lobate element (triangles in the middle of the figure represent the position of the log). Right log shows two lobe elements (triangles on the right show position of the log).

Fig. 9: (a) Photograph and correlation between DR6, 7 & 8 between the SW and NE faces of the ridge, showing down dip deepening and thickening of the channel. Palaeocurrents are parallel with the exposure. *1,2,3,4 mark key surfaces. (b) Geometrical relationships between channelised and lobate bodies from up-dip (SW) to down-dip (NE). Colour code as for Figure 3 and 6. Blue colour represents bidirectional measurements while green colour represents unidirectional measurements

Fig. 10: Walked out correlation between DR1, DR6 and the OUS section, 2 km down dip. The top of the OUS section is interpreted as turbidites deposited from flows that bypassed the channelised shelf-

edge rollover. Outcrop photographs (a) and (b) show details of the erosion down dip. Blue lines represent regional flooding surfaces and the red line is the correlation of the basal sequence boundary of the middle unit.

Fig. 11: a) Synthesis of observations and interpretations, showing generalised vertical and lateral stacking of depositional elements for a prograding mixed-influence shelf edge rollover. Note the stratigraphic decrease in channel size. b) Detail of a channel morphology in this setting.

Table 1: Facies classification, description and process interpretations of the middle unit.

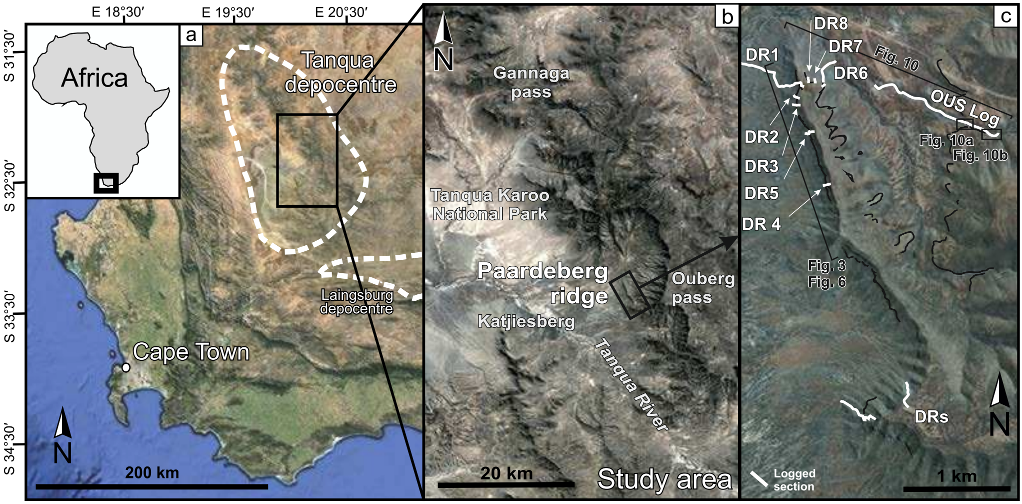

E 18°30′
E 19°30′
E 20°30′
S 31°30′
S 32°30′
S 33°30′
S 34°30′
a
Africa
Tanqua depocentre
Laingsburg depocentre
Cape Town
N
200 km
b
N
Gannaga pass
Tanqua Karoo National Park
Paardeberg ridge
Katjiesberg
Ouberg pass
Tanqua River
20 km
Study area
c
DR8
DR7
DR1
DR6
Fig. 10
OUS Log
DR2
DR3
DR5
DR 4
Fig. 10a
Fig. 10b
Fig. 3
Fig. 6
DRs
N
Logged section
1 km

Fig.1

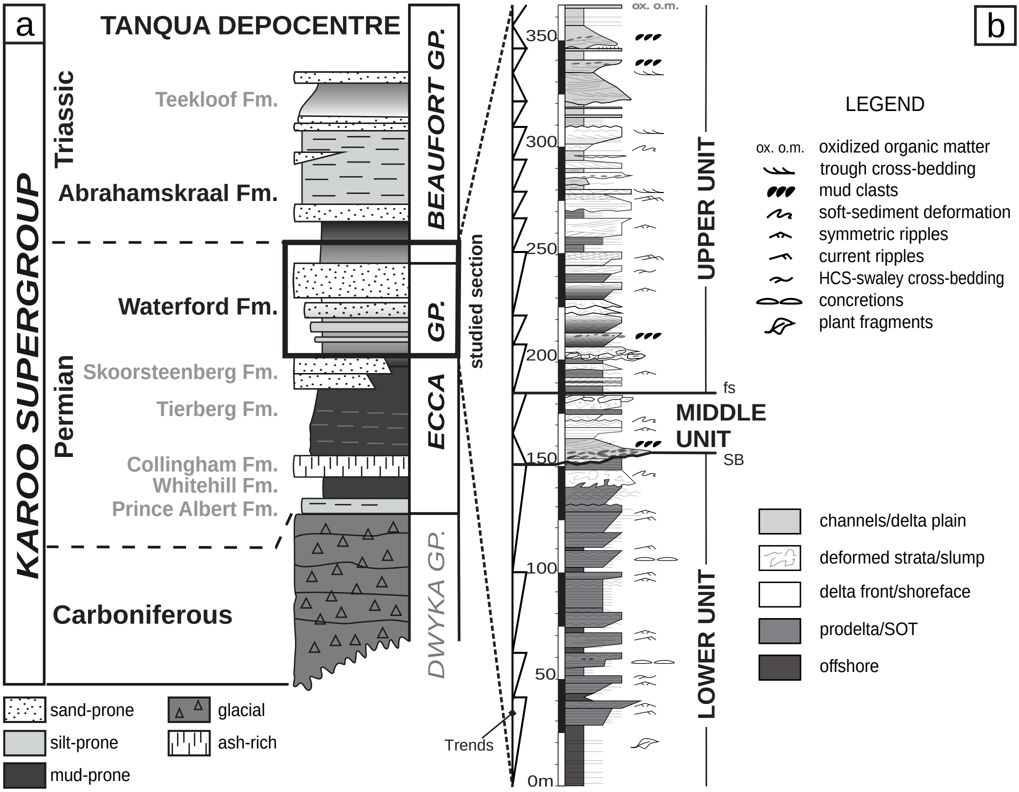
a
TANQUA DEPOCENTRE
KAROO SUPERGROUP
Triassic
Permian
Carboniferous
Teekloof Fm.
Abrahamskraal Fm.
Waterford Fm.
Skoorsteenberg Fm.
Tierberg Fm.
Collingham Fm.
Whitehill Fm.
Prince Albert Fm.
BEAUFORT GP.
GP.
ECCA
DWYKA GP.
studied section
sand-prone
silt-prone
mud-prone
glacial
ash-rich
b
ox. o.m.
350
300
250
200
150
100
50
0m
Trends
UPPER UNIT
fs
MIDDLE UNIT
SB
LOWER UNIT
LEGEND
ox. o.m. oxidized organic matter
trough cross-bedding
mud clasts
soft-sediment deformation
symmetric ripples
current ripples
HCS-swaley cross-bedding
concretions
plant fragments
channels/delta plain
deformed strata/slump
delta front/shoreface
prodelta/SOT
offshore

Fig.2

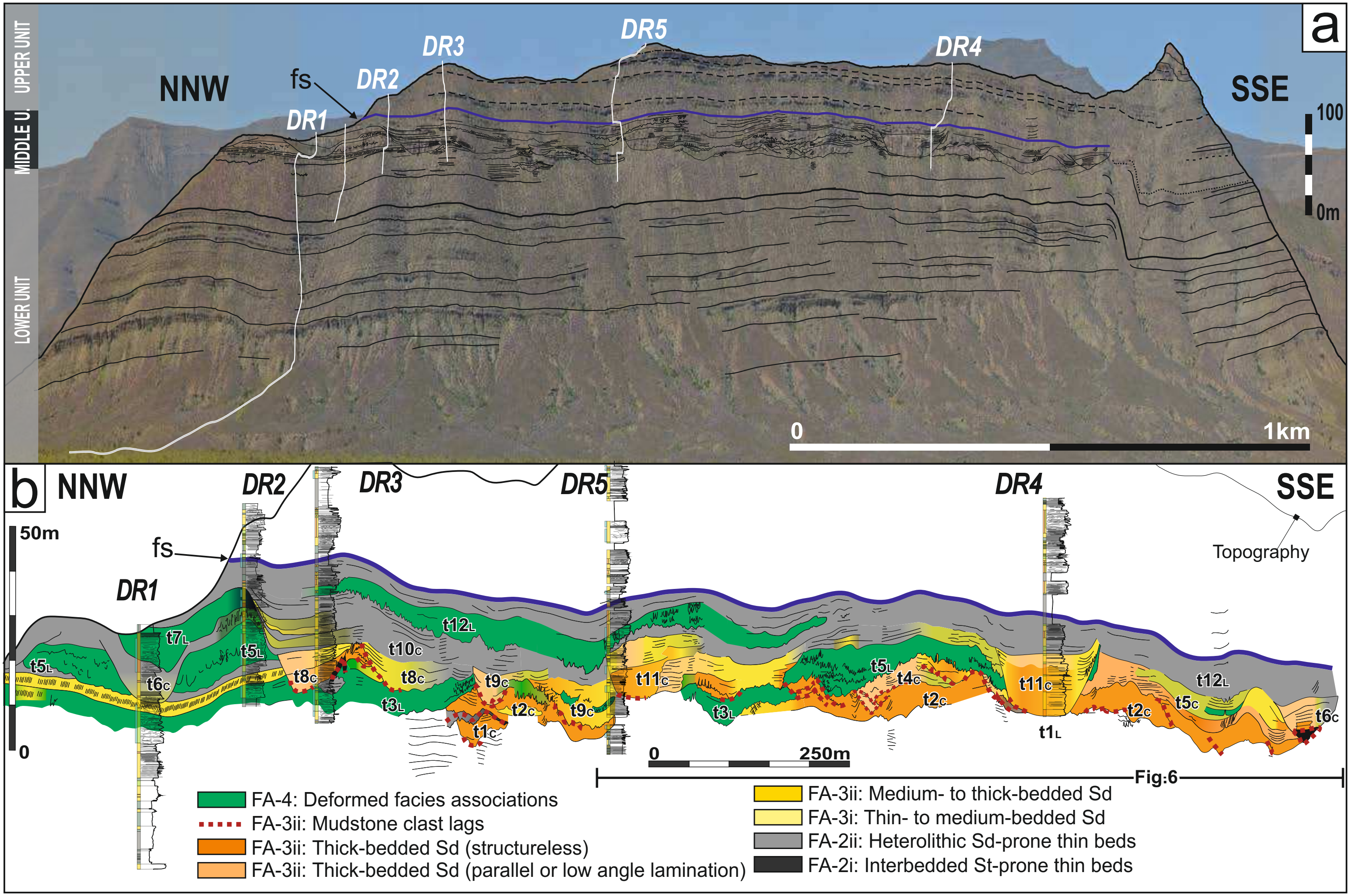
a
UPPER UNIT
MIDDLE U.
LOWER UNIT
NNW
SSE
fs
DR1
DR2
DR3
DR5
DR4
100
0m
0
1km
b
NNW
SSE
DR1
DR2
DR3
DR5
DR4
50m
0
fs
Topography
t5L
t6C
t7L
t8C
t3L
t10C
t12L
t9C
t1C
t2C
t11C
t4C
t1L
t5C
t6C
0
250m
Fig:6
FA-4: Deformed facies associations
FA-3ii: Mudstone clast lags
FA-3ii: Thick-bedded Sd (structureless)
FA-3ii: Thick-bedded Sd (parallel or low angle lamination)
FA-3ii: Medium- to thick-bedded Sd
FA-3i: Thin- to medium-bedded Sd
FA-2ii: Heterolithic Sd-prone thin beds
FA-2i: Interbedded St-prone thin beds

Fig.3

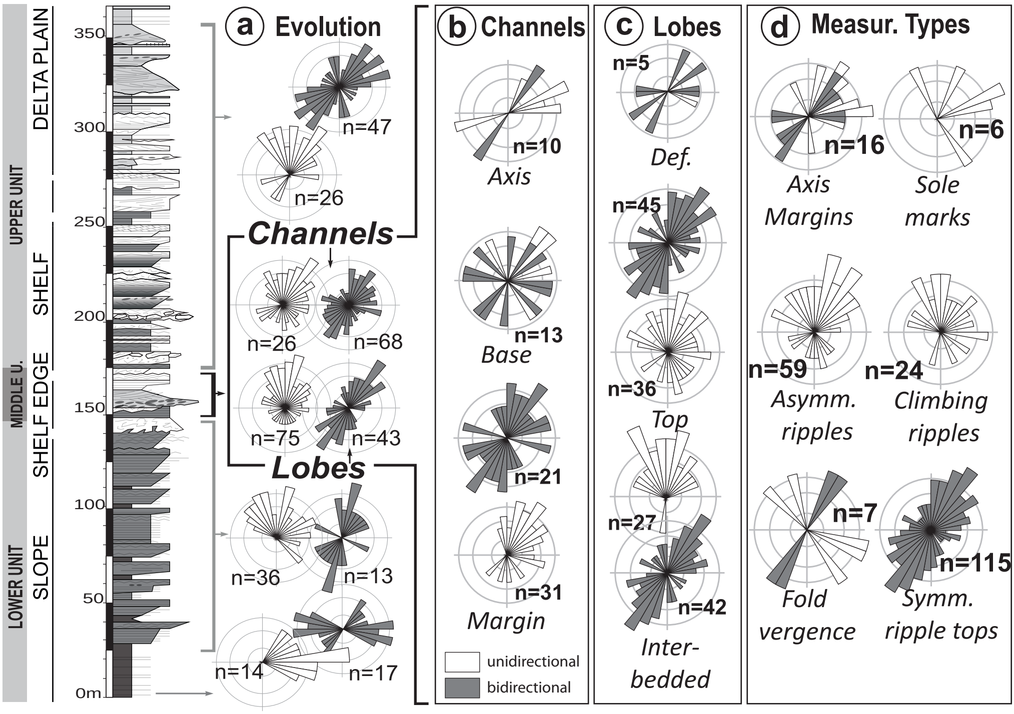

a Evolution
b Channels
c Lobes
d Measur. Types
DELTA PLAIN
SHELF
SHELF EDGE
SLOPE
UPPER UNIT
MIDDLE U.
LOWER UNIT
350
300
250
200
150
100
50
0m
n=47
n=26
Channels
n=26
n=68
n=75
n=43
Lobes
n=36
n=13
n=14
n=17
n=10
Axis
n=13
Base
n=21
n=31
Margin
unidirectional
bidirectional
n=5
Def.
n=45
n=36
Top
n=27
n=42
Inter-
bedded
n=16
Axis
Margins
n=6
Sole
marks
n=59
Asymm.
ripples
n=24
Climbing
ripples
n=7
Fold
vergence
n=115
Symm.
ripple tops

Fig.4

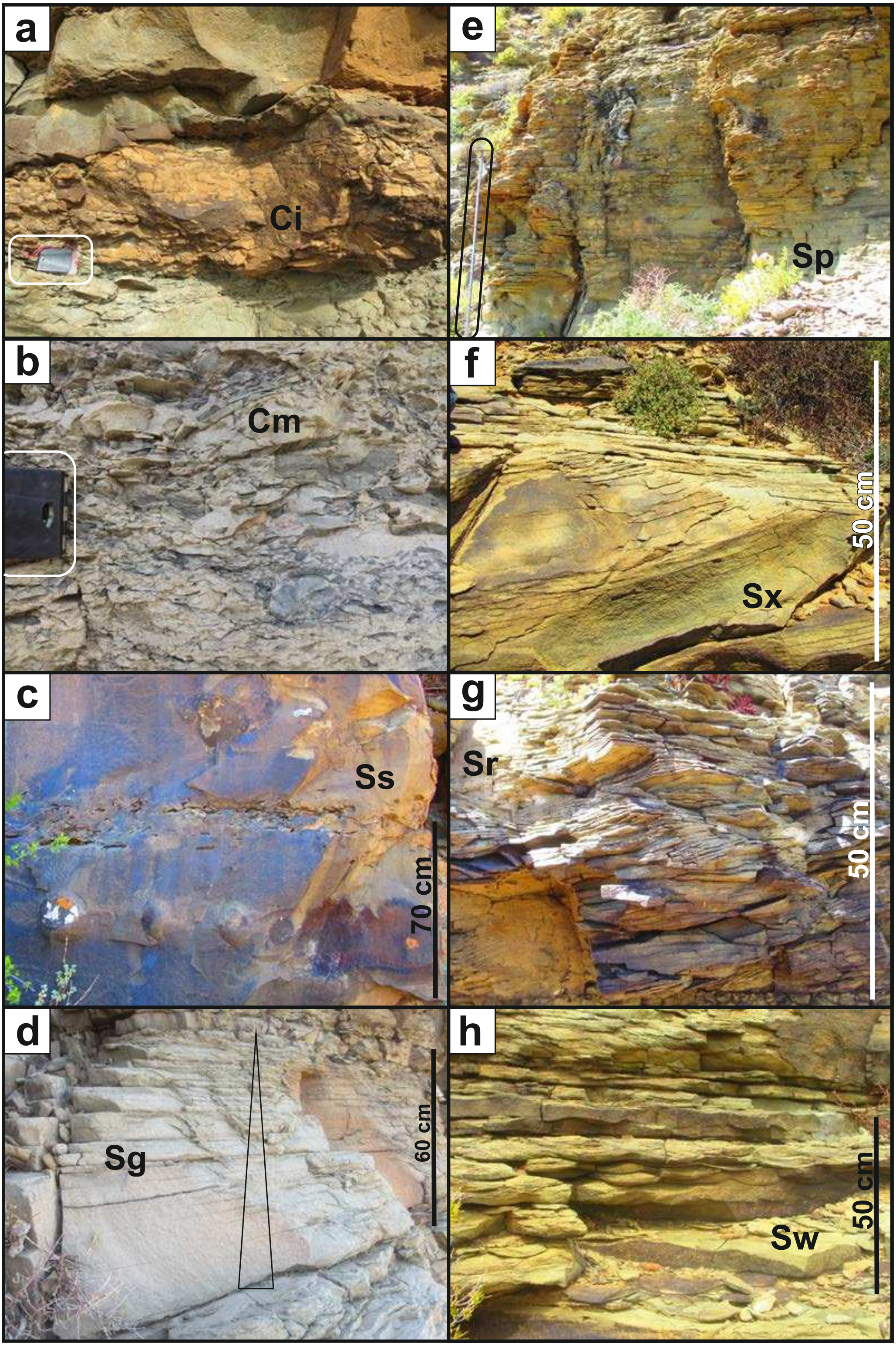

Fig5.

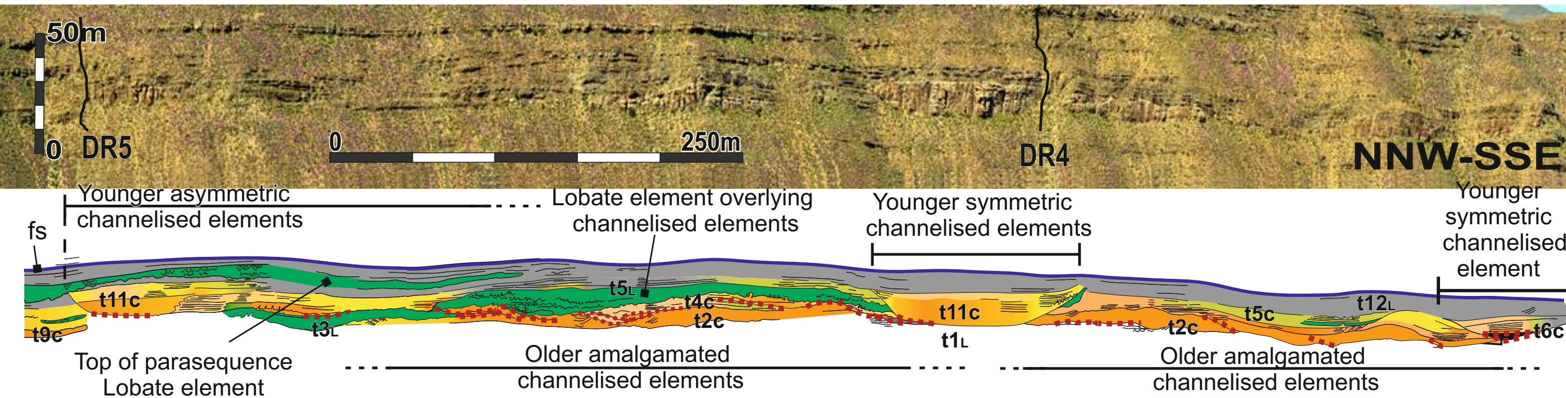

Dimensions - Channelised Elements												Mean
Time (t)	8	11	2	5	2	8	2	11	9	6	1	6	
WIDTH	>450	>350	>308	>158	>208	133	>133	128	>116	116	>75	75	187.5
THICKNESS	25	>10	>10	>10	>6	20	>7	25	>8	5	>10	15	12.58
LENGTH	-	>317	>362	-	>340	>357	-	>288	>304	>110	>340	-	201.5

Dimensions - Lobate Elements						Mean
Time (t)	12	3	5	5	7	
WIDTH	>667	>625	>408	>325	>168	400.2
THICKNESS	8	>5	>8	>10	>10	8.2

- FA-4: Deformed facies associations
- FA-3ii: Mudstone clast lags
- FA-3ii: Thick-bedded Sd (structureless)
- FA-3ii: Thick-bedded Sd (parallel or low angle lamination)
- FA-3ii: Medium- to thick-bedded Sd
- FA-3i: Thin- to medium-bedded Sd
- FA-2ii: Heterolithic Sd-prone thin beds
- FA-2i: Interbedded St-prone thin beds

Fig.6

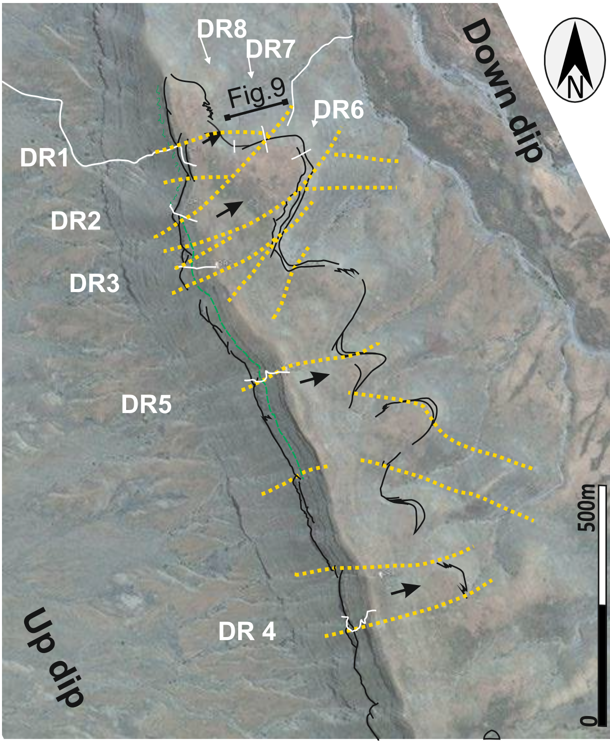

	Channels	
	SW	NE
	up dip	down dip
Thickness	thinner	thicker
Incision/ erosion	less deep	more deeply incised
Mud clast lags	less	more
Soft sediment deformation	less	more
Cutting/ Facies eroded	shallower facies: delta front or other channels	deeper facies: prodelta

Fig.7

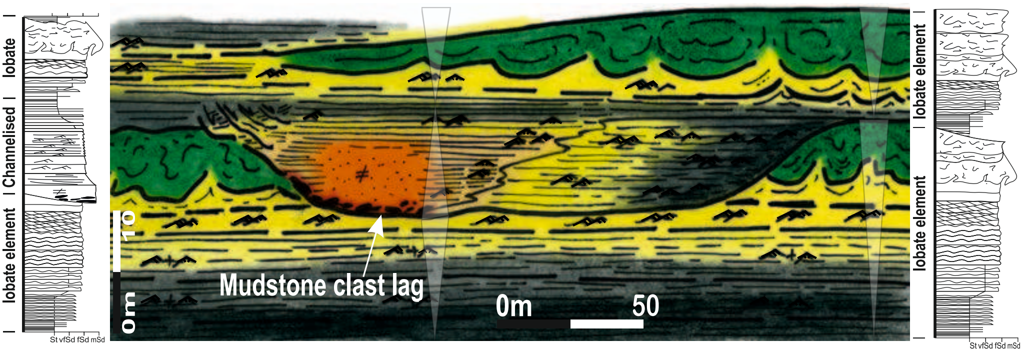
lobate
Channelised
lobate element
St vfSd fSd mSd
10
0m
Mudstone clast lag
0m
50
lobate element
lobate element
St vfSd fSd mSd

Fig.8

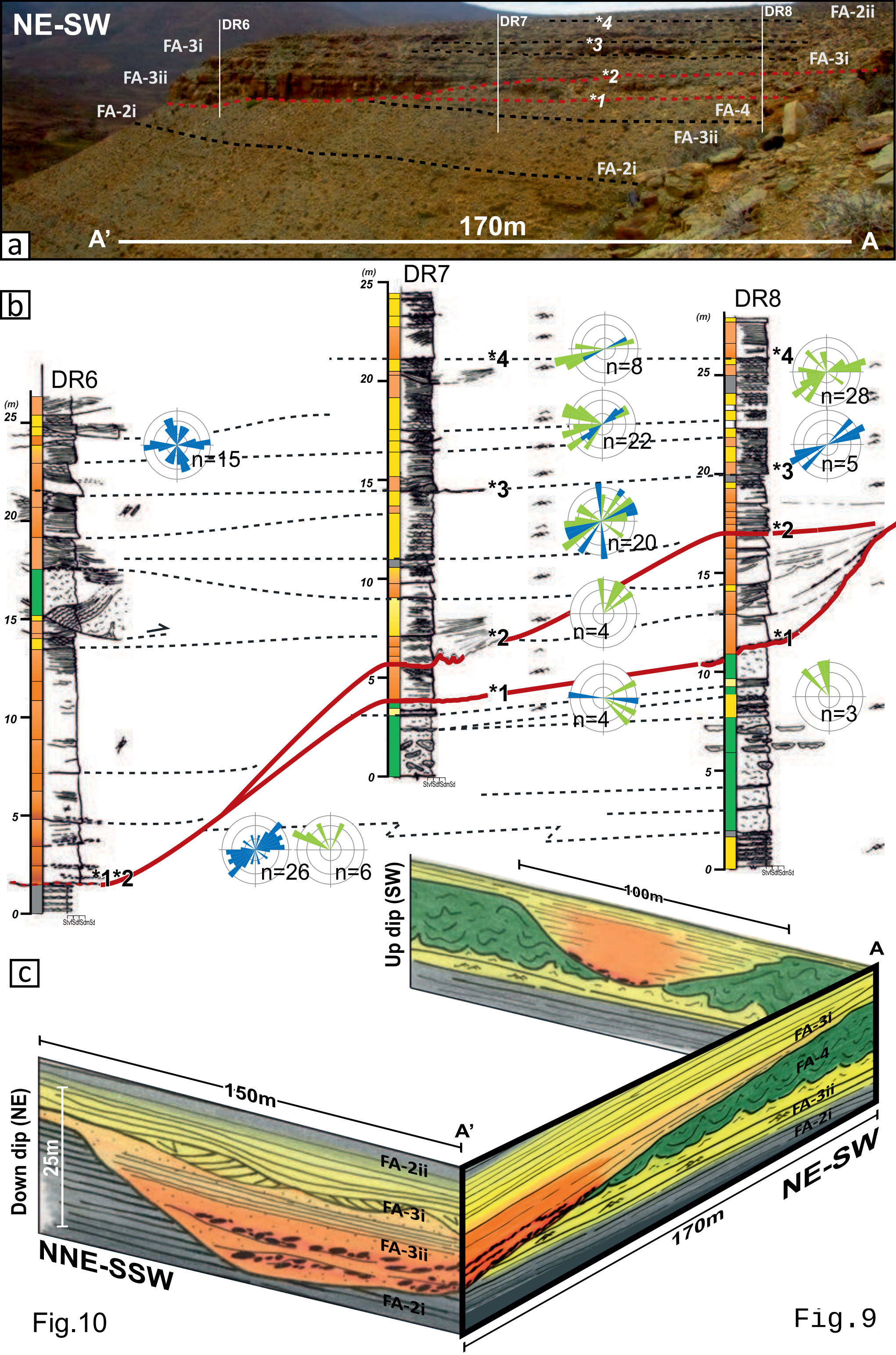

a
NE-SW
DR6
DR7
DR8
FA-3i
FA-3ii
FA-2i
FA-2ii
FA-4
*1
*2
*3
*4
A'
A
170m
b
DR6
DR7
DR8
(m)
n=15
n=8
n=22
n=20
n=4
n=4
n=28
n=5
n=3
n=26
n=6
StvfSdfSdmSd
c
Up dip (SW)
Down dip (NE)
100m
150m
25m
NNE-SSW
NE-SW
170m

Fig.10

Fig.9

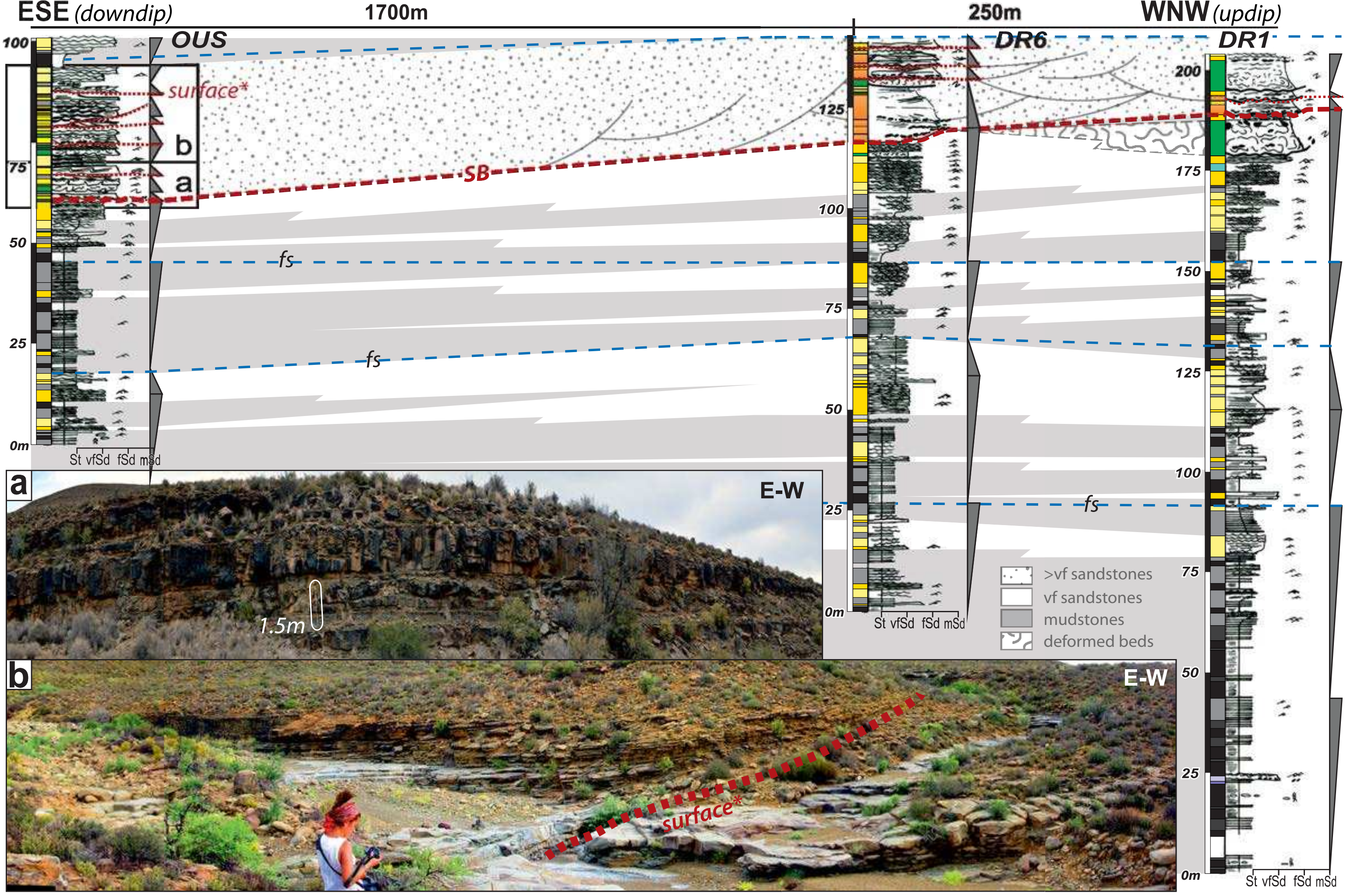

ESE (downdip)
1700m
250m
WNW (updip)
OUS
DR6
DR1
surface*
b
a
SB
fs
fs
fs
St vfSd fSd mSd
a
E-W
1.5m
b
E-W
surface*
>vf sandstones
vf sandstones
mudstones
deformed beds

Fig.10

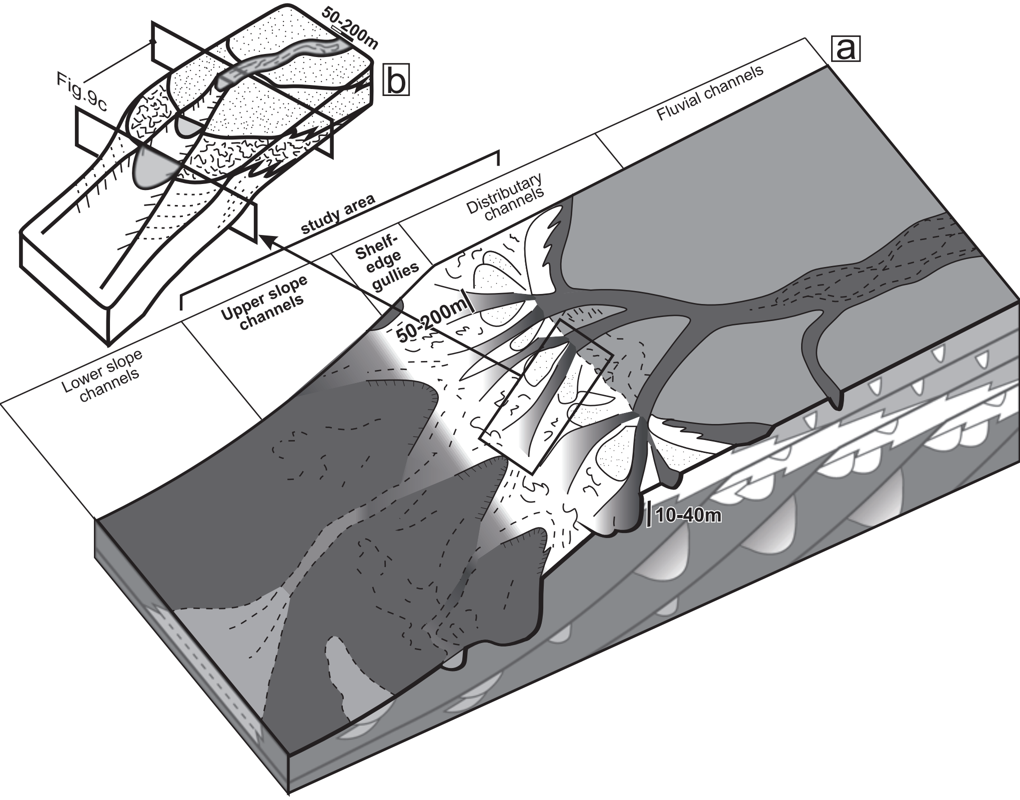

50-200m
b
Fig.9c
a
Fluvial channels
study area
Distributary channels
Shelf-edge gullies
Upper slope channels
50-200m
Lower slope channels
10-40m

Fig.11

	Lithofacies	Sedimentary structures	Thickness, lithology and textural properties	Process interpretation	Other characteristics	FA
Conglomerate facies (C)	Ci	Matrix- to clast-supported intraformational conglomerate, crudely cross-stratified	cm- to dm- scale, poorly-sorted and matrix- to clast-supported intraformational conglomerate. Siltstone to sandstone matrix, with mudstone, siltstone or sandstone clasts, 0.5-20 cm in diameter. Irregular contacts, commonly erosive bases, poorly formed cross-bedding and gradational tops (Fig.5a).	Locally sourced lithic clasts transported as bedload and deposited as basal lag when flow loses energy. Cross-bedding indicates migration of dunes and bars. Outsize clast content suggests bank collapse and erosion during high energy flows, or channel lateral migration.	Reddening of lags may represent oxidation of iron-rich minerals.	FA-3ii
	Cm	Mudstone clast horizon	Horizons of claystone and siltstone rip-up clasts within fine- or medium-grained sandstone beds. Clasts are up to 20 cm in size, rounded to angular and typically poorly-sorted. Beds are irregular in thickness and often erosional (Fig.5b).	Mudstone clasts entrained from erosion of underlying claystone and siltstone material during scour. Where mudstone clast horizons occur amongst sandstones, this is interpreted as high magnitude, low frequency flows, mobilising the mudstone clasts.	Mud clasts are commonly aligned or imbricated.	FA-3ii
Sandstone facies (S)	Ss	Structureless	cm- to m-scale poorly to moderately-sorted very fine to medium-grained sandstone. Sharp base and top, rarely erosive. Few gradational tops (Fig.5c).	*En masse* deposition from high velocity and density sediment gravity flows. Uniform narrow grain size range suggests rapid deposition under upper flow regime conditions also supressing bedform development.	Internal structures overprinted by intensive bioturbation or dewatering. Locally abundant in plant remains and oxidized organic matter.	FA-2, FA-3, FA-4
	Sg	Inverse or normal grading	cm- to m-scale moderately to well-sorted very fine to fine, or medium-grained sandstone. Base and top can be either sharp or gradational (Fig.5d).	Normal grading interpreted to reflect evidence of waning flow conditions. Inverse grading reflects waxing flow conditions attributed to river floods.	Plant debris and mica, and development of composite reverse-graded to graded beds.	FA-2, FA-3, FA-4
	Sp	Parallel bedding	cm- to m-scale moderately to well-sorted very fine to fine-grained sandstone. Sharp top and base, rarely erosive or gradational. Parting lineations are common (Fig.5e).	Deposition under upper phase plane bed conditions. Parting lineations can be produced by turbulent eddies or microvortices at the bed boundary layer. Also interpreted as representing vertical aggradation under shallow flow conditions.	Parting lineation, mud clasts, oxidized organic matter and plant fragments observed in parallel laminas	FA-2, FA-3, FA-4
	Sl	Low angle cross-bedding, SCS or HCS	cm- to m-scale well sorted very fine to fine-grained sandstone. Sharp base and top, rarely erosive. Commonly features undulatory bed tops.	Deposited under low flow regime conditions within large-scale dunes and barforms. Interpreted as representing deposition in broad bedload sheets, during migration downstream, and affected by combined or oscillatory flows.	Well-sorted rounded grains, mud clasts associated to erosive bases and common symmetrical-rippled tops.	FA-2, FA-3, FA-4
	Sx	High angle planar or trough cross-bedding	cm- to m-scale moderately-sorted very fine to medium-grained sandstone. Sharp base and top, rarely erosive. Few gradational tops (Fig.5f).	Planar cross-stratification represents migration of 2-D subaqueous dunes interpreted to represent deposition within deeper and/or faster parts of a confined/channelized flow. Trough cross bedding is interpreted to reflect migration of 3-D dunes through bedload transportation. 3-D dunes occur under lower flow regime conditions, where deeper scours are most prevalent, and are associated with both downstream and laterally accreting barforms.	Mud clasts, oxidized organic matter and plant fragments are observed in cross-sets.	FA-3, FA-4
	Sr	Ripple or climbing ripple-lamination	mm- to dm-scale moderately-sorted very fine to fine-grained sandstone. Generally sharp or gradational bases and asymmetrical rippled tops (Fig.5g).	Tractional bedforms developed under lower flow regime conditions. Asymmetrical current ripples produced by uni-directional flows. Climbing ripples reflecting higher sedimentation rates.	Ripples locally show stoss and lee side preservation.	FA-2, FA-3, FA-4
	Sw	Wavy lamination and symmetrical ripple-lamination	mm- ro dm-scale well-sorted very fine to fine-grained sandstone. Generally sharp or gradational bases and symmetrical rippled tops (Fig.5h).	Tractional bedforms developed under lower flow regime conditions, with symmetrical crests created by bi-directional currents under orbital wave motion. Secondary ladder-back ripple sets formed between larger ripple troughs.	Well-sorted, rounded grains. Common superimposition of interference ripples.	FA-2, FA-3, FA-4
Mudstone facies (M)	Ms	Parallel to ripple-laminated, normally and inversely-graded fissile siltstones and mudstones	mm- to dm-scale poorly to moderately-sorted coarse siltstone beds. Contacts are generally gradational. Locally sharp based.	Deposition from very low-density turbidity/hyperpycnal currents, sometimes associated with river floods or storms. Post depositional compaction masks primary sedimentary structures.	Common appearance of starved and lenticular unidirectional ripples.	FA-1, FA-2, FA-4
	Md	Dark grey to black structureless siltstones and mudstones	mm- to m-scale moderately to well-sorted medium to fine siltstone beds. Generally gradational contacts, locally sharp.	Hemipelagic fall-out from low current velocities or low suspended sediment concentrations during conditions of low clastic input. Mode of deposition ensures regional coverage of the mudstone deposits in distal settings.	Often associated with sideritic concretionary horizons.	FA-1, FA-2, (FA-4)
	Mo	Light grey to olive green, structureless to well laminated siltstones and mudstone	cm- to m-scale poorly to moderately-sorted coarse to fine siltstone beds. Generally gradational contacts, locally sharp.	Deposition by direct fallout from suspension, or debris-flows leading to a structureless appearance. Green colouration indicates waterlogged environment.	Local development of carbonate-rich nodular levels.	FA-1, (FA-2)

Table.1